AIDS RESEARCH AND HUMAN RETROVIRUSES
Volume 25, Number 9, 2009

DOI: 10.1089/aid.2009.0036

Short Communication: Generation of Recombinant Monoclonal Antibodies against an Immunodominant HLA-A*2402-Restricted HIV Type 1 CTL Epitope

Jun-ichi Nunoya,[1] Toshihiro Nakashima,[2] Ai Kawana-Tachikawa,[1] Katsuhiro Kiyotani,[3] Yuji Ito,[4] Kazuhisa Sugimura,[4] and Aikichi Iwamoto[1,5,6]

Abstract

Molecular interaction between the peptide/MHC class I complexes (pMHCs) and T cell receptor (TCR) is fundamental to the effector function of cytotoxic T lymphocytes (CTLs). Monoclonal antibody against pMHC with TCR-like specificity is a possible research tool for the antigen presentation. However, it is notoriously difficult to isolate monoclonal antibodies against pMHCs by the conventional hybridoma technique. To isolate monoclonal antibodies against an immunodominant HIV-1-derived CTL epitope in the *nef* gene, we panned phage clones from a human scFv phage display library. Eight Nef138-10/HLA-A*24(A24)-specific scFv clones were isolated and two of them (scFv#3 and scFv#27) were selected for further analysis. The clones stained A24-positive cells pulsed with Nef138-10 peptides specifically. We reconstituted humanized immunoglobulin Gs (IgGs) using a baculovirus expression system. Reconstituted IgGs kept the original specificities of the parental scFvs. The dissociation constants were 23 μM and 20 μM by Biacore, respectively. This is the first report of a successful generation of monoclonal antibodies against an HIV-1 CTL epitope loaded on an MHC class I molecule.

Cellular immune response by cytotoxic T lymphocytes (CTLs) is a critical line of host defense against human immunodeficiency virus type 1 (HIV-1).[1] The first step in the CTL-based immune response is CTL activation, which is triggered through antigen recognition by a clonotypic T cell receptor (TCR).[2,3] Rather than binding to the viral antigen itself,[4] TCR binds to a complex formed with HIV-1-derived peptides and major histocompatibility complex (MHC) class I molecules (pMHCs).[5,6] Due to viral strategies to evade immune recognition, the CTL-based immune response is only partially effective in suppressing HIV-1.[1,7] One of the mechanisms by which HIV-1 circumvents CTL activities is through downregulation of MHC class I molecules by the viral Nef protein.[8] Emergence of escape mutations that alter pMHC binding or recognition is another viral strategy to disrupt the CTL-based immune response.[9,10] We previously reported that stereotypic Y to F (Y139F) substitution at the second position in an immunodominant HLA-A*2402(A24) restricted CTL epitope in the Nef protein (Nef138-10; RYPLTFGWCF) has an escape phenotype and is becoming widespread in the Japanese population.[11]

To understand cellular immune responses against HIV-1 infection, both antigen presentation and cellular responses should be analyzed. A decade ago, Altman *et al.* developed a system to analyze and evaluate the phenotype of antigen-specific T lymphocytes using pMHC tetramers.[12] However, relatively few studies have been performed to examine antigen presentation at cellular and molecular levels. For example, pMHCs derived from infecting HIV-1 have been analyzed indirectly by mass spectrometry and Cr release assays.[13,14] Lack of a suitable reagent has precluded the direct visualization and quantification of pMHCs derived from infecting HIV-1. Antibodies against HIV-1-specific pMHCs could be a useful tool to analyze antigen presentation both qualitatively

[1]Division of Infectious Diseases, Advanced Clinical Research Center, The Institute of Medical Science, The University of Tokyo, Tokyo, Japan.
[2]Division 2, First Research Department, Kikuchi Research Center, The Chemo-Sero-Therapeutic Research Institute, Kumamoto, Japan.
[3]Department of Virology, Graduate School of Biomedical Sciences, Hiroshima University, Hiroshima, Japan.
[4]Department of Bioengineering, Faculty of Engineering, Kagoshima University, Kagoshima, Japan.
[5]Research Center for Asian Infectious Diseases, The Institute of Medical Science, The University of Tokyo, Tokyo, Japan.
[6]Department of Infectious Diseases and Applied Immunology, Research Hospital, The Institute of Medical Science, The University of Tokyo, Tokyo, Japan.

and quantitatively, and the molecular interaction between pMHC and their ligands. In other studies, monoclonal antibodies against pMHCs have been isolated for specific combinations of peptides and MHC class I molecules.[15,16] In earlier studies using hybridoma technology, we attempted to isolate pMHC antibodies but failed. Technical difficulties of raising antibodies against pMHCs using a conventional hybridoma technique has led to the development of phage display techniques to isolate pMHC-specific antibodies.[17,18] We and others have constructed large phage display libraries that can be used to isolate rare antibodies.[19–21] In recent years, several recombinant antibodies against pMHC with TCR-like specificity have been isolated from similar human antibody libraries.[18,22–24] To investigate the mechanism for the escape phenotype associated with the Nef138-10 epitope at a molecular level, we tried to raise monoclonal antibodies against the epitope using the phage display technique.

We produced soluble Nef138-10/A24 and Env584-11/A24 using a Sendai virus expression system. These molecules were purified from the supernatant, and biotinylated with BirA enzyme as described previously.[25] To select Nef138-10/A24 antibodies, we used pooled human single-chain fragment variable (scFv) phage display libraries.[19] This pooled scFv library consists of four scFv library Vγ–Vλ, Vγ–Vκ, Vμ–Vκ, and Vμ–Vλ, containing 1.1×10^8, 2.1×10^8, 8.4×10^7, and 5.3×10^7 independent clones, respectively. To remove phages that might bind nonspecifically to the beads, the library (1.0×10^{12} transforming units) was incubated with streptavidin-coated magnetic beads (Dynal, Oslo, Norway) for 1 h with continuous rotation. The beads were removed and the supernatant was incubated for 1 h with 500 nM Nef138-10/A24s. Streptavidin-coated magnetic beads were incubated for 1 h with 2% skim milk/phosphate-buffered saline (PBS) and then added to the antigen/supernatant mixture. After a 15-min incubation with continuous rotation, the supernatant was removed and the beads were washed 10 times with PBS containing 0.1% Tween 20 and two times with PBS. Phages were eluted from the beads with 100 mM triethylamine (Sigma, St. Louis, MO), and the solution was immediately neutralized by the addition of 1 M Tris–HCl (pH 7.4). *Escherichia coli* strain TG1 (GE Healthcare UK Ltd.) was transduced with eluted phages and plated on a 2xYT agar plate containing 2% glucose and 100 μg/ml carbenicillin (Sigma). After overnight incubation at 30°C, all colonies were picked and cultured in a single flask with liquid medium, with the addition of helper phage M13KO7 (GE Healthcare UK Ltd.). The scFv-displayed phages were purified from the supernatant by polyethylene glycol precipitation, titrated with *E. coli* strain TG1, and used for the next round of panning.

The protocol for the second and third rounds was the same as for the first round, except that phage supernatant was incubated with a lower concentration (100 nM) of Nef138-10/A24 peptide complexes. After two and three rounds of panning the scFv phage display library with biotinylated Nef138-10/A24 and streptavidin-coated magnetic beads in solution, we achieved a 38.2- and 4200-fold enrichment, respectively, for scFvs that bind to Nef138-10/A24 (Fig. 1A).

After the third round of panning, helper phages were added to each culture of the individual colonies in order to recover phages for ELISA as described previously.[23] Briefly, 96-well maxisorp plates (Nunc, Rochester, NY) were coated with biotinylated bovine serum albumin (BSA) (1 μg/well; Vector Laboratories Inc., Burlingame, CA) overnight at 4°C, washed three times with 0.1% Tween 20/PBS (the buffer used for all subsequent washes), and incubated with streptavidin (1 μg/well; Sigma) for 1 h. Plates were washed three times, incubated with biotinylated peptide/A24 (0.5 μg/well) for 1 h, and blocked with 2% skim milk/PBS for 30 min. Plates were washed three times, incubated for 1 h with $\sim10^{10}$ phages or isolated antibodies, and washed three times. Detector antibodies were added (see figure legends) and plates were incubated for 1 h at 4°C. Plates were washed four times, and antibody binding was detected by a colorimetric detection method with a TMB reagent (Pierce Biotechnology Inc., Rockford, IL). The reaction was stopped by the addition of 0.5 M H_2SO_4. In addition, DNA fragments encoding scFv were amplified by colony PCR with primers C5E-S1 (5′-CAACG TGAAAAAATTATTATTCGC-3′) and C5E-S6 (5′-GTAAAT GAATTTTCTGTATGAGG-3′). DNA sequencing was performed using the same primers and the ABI Prism dye terminator cycle sequencing Ready Reaction kit (Applied Biosystems, Foster City, CA) on a Perkin-Elmer ABI-377 sequencer. We isolated 80 clones of scFv-displaying phages after the third round of panning and assayed them by ELISA to assess binding to Nef138-10/A24 and Env584-11/A24 (Fig. 1B). As a control, we used the monoclonal antibody W6/32, which binds to HLA-ABC molecules properly associated with a heavy chain and a β_2-microglobulin. W6/32 recognized both Nef138-10/A24 and Env584-11/A24, indicating that both peptide/A24 complexes maintained a correct conformation during the ELISA procedure (Fig. 1B, PC).

Of the 80 clones, 16 bound preferentially to Nef138-10/A24; the remainder bound to both Nef138-10/A24 and Env584-11/A24. Following *Bst*OI digestion and sequencing of the 16 scFv DNA fragments that were specific for Nef138-10/A24, we isolated eight independent clones of scFv-displaying phages. We confirmed the expression and binding specificity of each scFv clone by Western blotting and ELISA with anti E-tag antibody.

For purification and detection of soluble scFvs, we genetically converted the E-tag located at the scFv C-terminus to the tandem sequences of c-Myc and 6xHis tags. To express scFvs, *E. coli* strain TG1 transformants were cultured at 30°C. When the OD_{600} reached 0.5, expression was induced by the addition of 1 mM IPTG. Cultures were incubated for an additional 4 h at 30°C. To prepare periplasmic fractions, bacteria were collected by centrifugation and osmotically shocked with ice-cold 0.2 M Tris–HCl containing 0.5 mM EDTA and 0.5 M sucrose at pH 8.0. scFvs were purified from periplasmic extracts by affinity chromatography with HiTrap Chelating HP Column (GE Healthcare UK Ltd.). After replacing the C-terminal E-tags with c-Myc and 6xHis tags, we confirmed the expression of each scFv clone in the periplasm and supernatant using Western blotting with anti c-Myc tag antibody (data not shown). We selected scFv#3 and scFv#27 for further analysis. In ELISA with anti-c-Myc tag antibody, soluble forms of scFv#3 and scFv#27 bound specifically to Nef138-10/A24 (Fig. 1C).

To analyze the binding specificity of the two selected scFv clones toward pMHCs expressed on the cell surface, we performed flow cytometry analysis of a peptide pulsed A24-positive Epstein–Barr virus-transformed B lymphoblastoid cell line (B-LCL) previously established in our laboratory.[25] Two$\times10^6$ cells from an A24-positive B-LCL were pulsed for 20

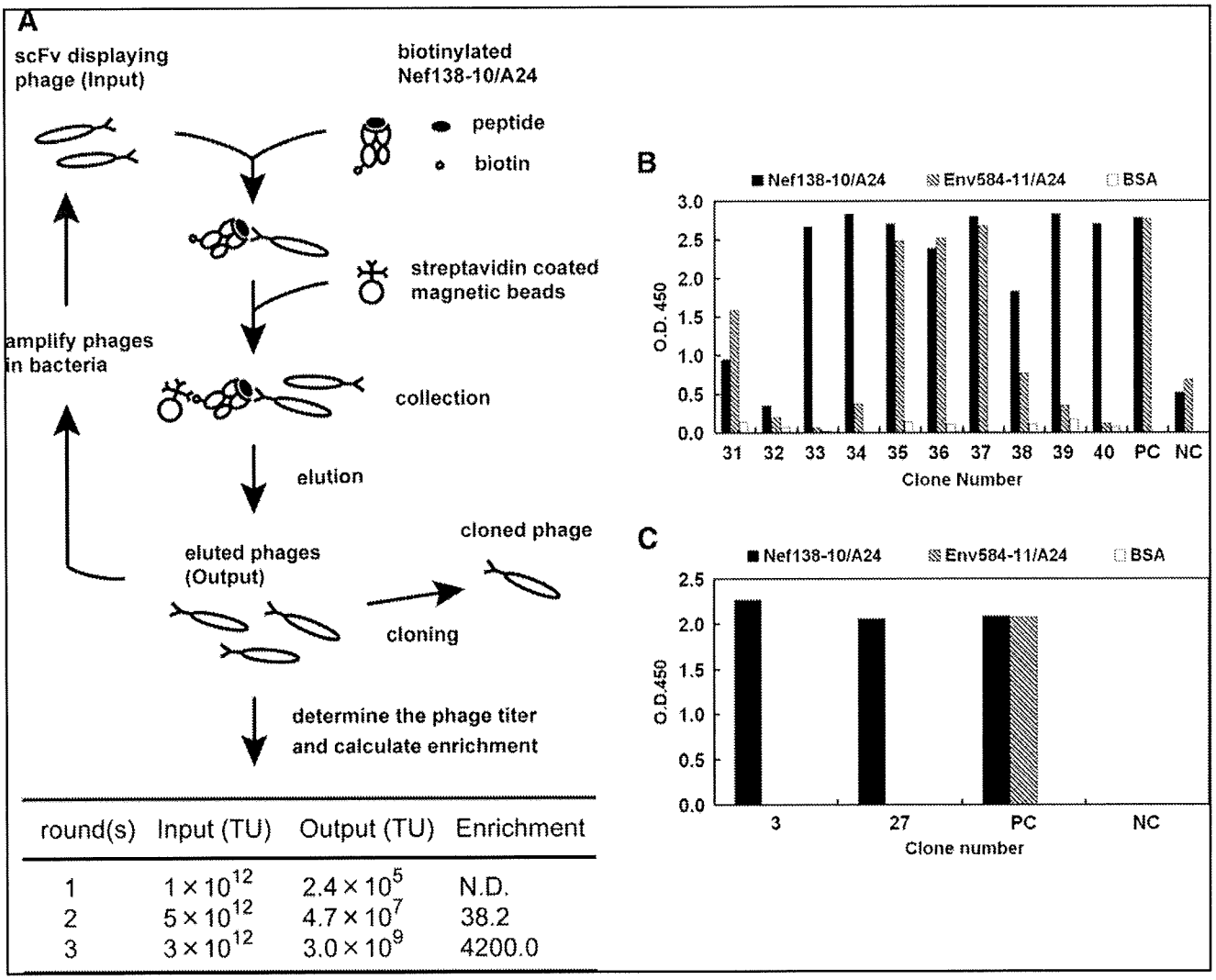

round(s)	Input (TU)	Output (TU)	Enrichment
1	1×10^{12}	2.4×10^{5}	N.D.
2	5×10^{12}	4.7×10^{7}	38.2
3	3×10^{12}	3.0×10^{9}	4200.0

FIG. 1. Isolation of scFvs directed against Nef138-10/A24. (**A**) A schematic representation of panning. The scFv-displaying phages that bind to Nef138-10/A24 were panned from a naive human scFv phage display library and collected by streptavidin-coated magnetic beads. Panning was repeated three times. The enrichment during panning was calculated from the phage titer bound to Nef138-10/A24. (**B**) Binding specificity of scFv-displaying phage clones from the phage pool after three rounds of panning. Recovered panned phages were screened in ELISA for specific binding to Nef138-10/A24 by using an HRP-conjugated anti-M13 phage antibody (GE Healthcare UK Ltd.). Each clonal phage and PBS as a negative control (NC) were assayed in duplicate for its binding to Nef138-10/A24 (filled bar), Env584-11/A24 (hatched bar), and BSA (open bar). We used an anti-HLA-ABC antibody (W6/32) as a positive control (PC), and detected the bound antibodies with HRP-conjugated antimouse immunoglobulins (Igs) antibodies (DAKO, Glostrup, Denmark). The numbers below the horizontal line indicate clones. The ordinate indicates the optical density value at 450 nm (OD_{450}). This figure shows results of typical 10 clones (scFv#31–40). We judged a clone specific binding to Nef138-10/A24, when its OD_{450} value of Nef138-10/A24 was 10 and 5 times higher than those of BSA and Env584-11/A24, respectively. (**C**) Binding specificity of scFvs expressed in the *E. coli* periplasm was analyzed by ELISA with anti-c-Myc-tag antibody (Santa Cruz Biotechnology Inc., Santa Cruz, CA).

to 24 h with 10 μM of each peptide in FCS-free RPMI. After pulsing, cells were washed three times, incubated with purified scFvs (50 μg/mL) for 1 h at 4°C, washed two times, and incubated with a biotinylated rabbit polyclonal anti-c-Myc antibody (10 μg/mL) for 1 h at 4°C. Cells were washed twice and incubated with R-phycoerythrin (PE)-conjugated streptavidin (10 μg/ml; BD Pharmingen, San Diego, CA) for 1 h at 4°C, then washed three times and fixed with PBS containing 1% paraformaldehyde. PBS containing 2% heat-inactivated normal rabbit serum (NRS) and 0.02% sodium azide was used as the diluent for all scFvs and antibodies. All washes were performed with PBS. Flow cytometry was performed using a FACSCalibur (BD Bioscience, San Jose, CA). Both scFv clones bound specifically to Nef-138-10/A24. No cross-reactivity was observed toward endogenously expressed HLA-A, HLA-B, or HLA-C molecules or toward A24-bound HIV-1 Gag28-9, HIV-1 Env584-11, or CMV pp65 complexes (Fig. 2). HLA-A, HLA-B, and HLA-C molecules were expressed equally among the cell populations used in this assay (Fig. 2, W6/32). These data suggest that the scFv#3 and scFv#27 bind specifically to

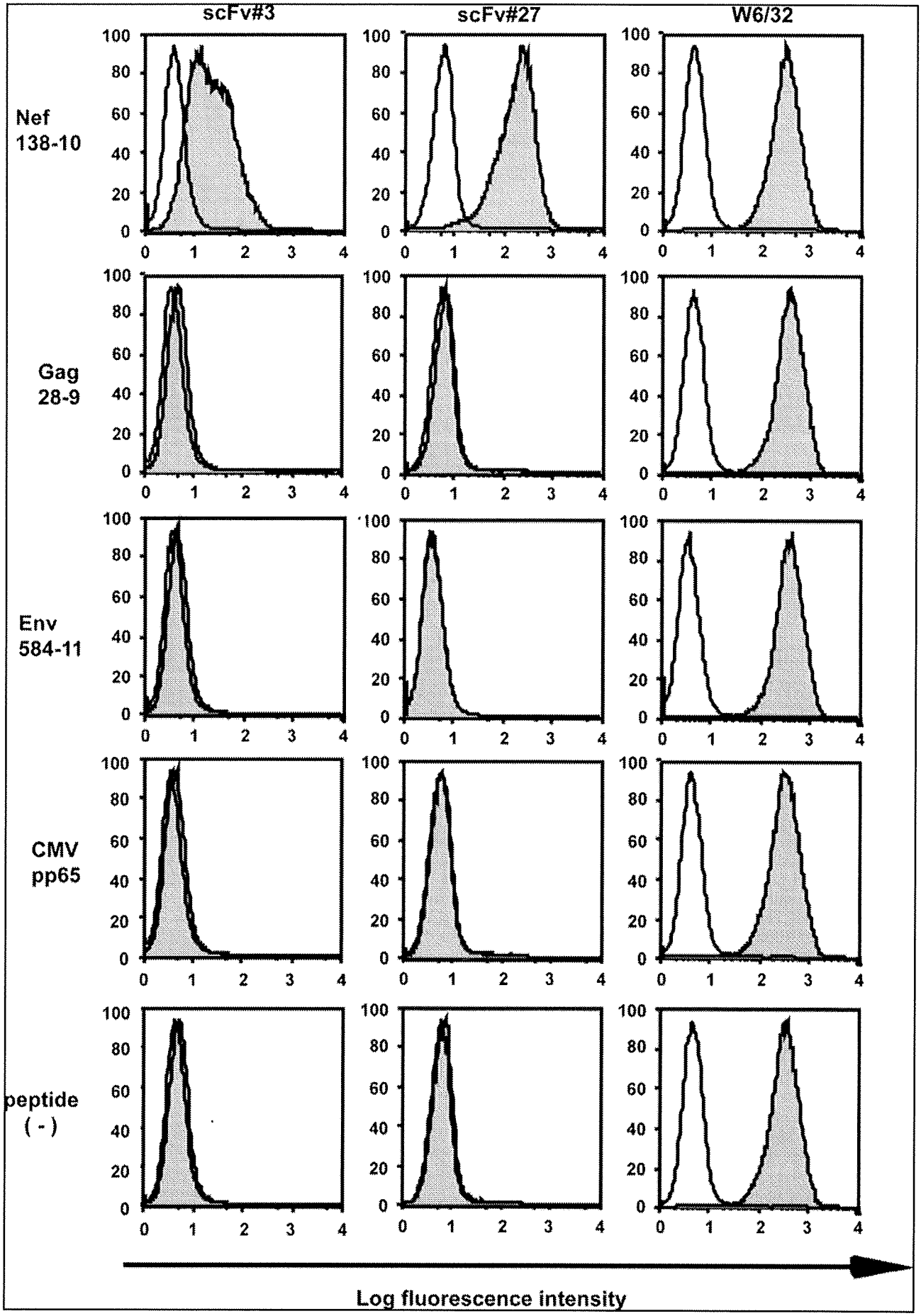
scFv#3
scFv#27
W6/32
Nef
138-10
Gag
28-9
Env
584-11
CMV
pp65
peptide
(-)
100
80
60
40
20
0
0 1 2 3 4
Log fluorescence intensity

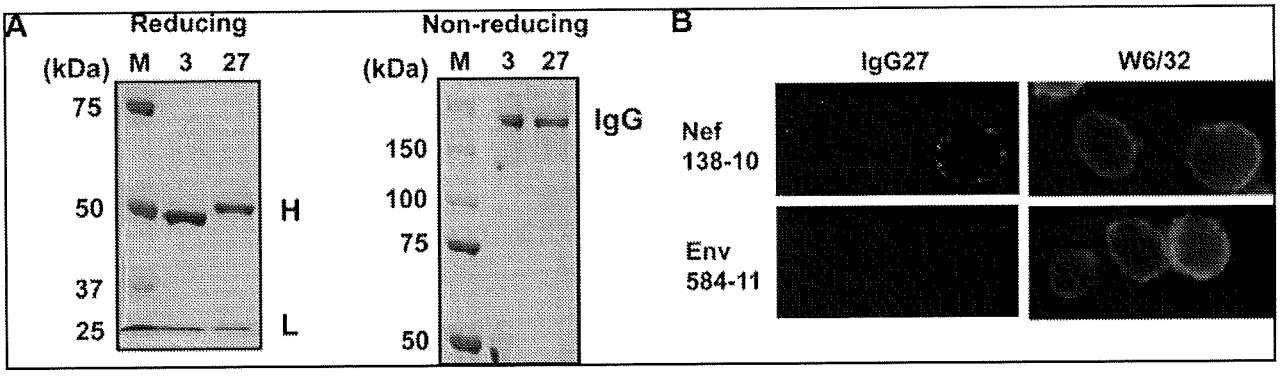

FIG. 3. Reconstitution of intact human IgG molecules by a baculovirus expression system. (**A**) CBB staining of expressed human IgG molecules under reducing and nonreducing conditions. Heavy and light chains are indicated by H and L, respectively. (**B**) A24-positive B-LCL cells were pulsed with 10 μM Nef138-10 or Env584-11 peptides, and stained with the reconstituted human IgG27. These cells were then stained with a biotinylated polyclonal rabbit anti-c-Myc-tag antibody (Santa Cruz Biotechnology Inc.), and finally with a PE-conjugated streptavidin. We also stained the cells with a PE-conjugated anti-HLA-ABC antibody (W6/32) to analyze the expression of HLA-ABC molecules on the cell surface. The stained cells were mounted and observed with an Eclipse E600 microscopy system. Two or three cells are shown in each image.

Nef138-10/A24 on the cell surface. The mean intensity of the fluorescent staining with scFv#27 was higher than the mean intensity seen with scFv#3 (Fig. 2, top panel).

Individual scFv clones were then converted to intact human IgG using the Bac-to-Bac Baculovirus expression system (Invitrogen Corporation, Carlsbad, CA). The human IgG1 heavy chain and Ig light chain expression cassettes from pAc-λ-CH3 and pAc-κ-CH3, respectively (PROGEN, Heidelberg, Germany), were inserted into pFastBac Dual under the polyhedrin promoter (light chain) and the p10 promoter (heavy chain). The VH and VL regions of each clone were inserted with the *ScaI*/*Hin*dIII site and *XhoI*/*Nhe*I site, respectively. Recombinant baculovirus was made according to the manufacturer's procedure. Titers were determined using the BacPAK Baculovirus Rapid Titer Kit (Clontech Laboratories, Inc., Mountain View, CA). Insect cells (Sf9 and High Five cells) were infected with recombinant baculovirus at a multiplicity of infection (MOI) of 5 and incubated for 96–120 h. In preliminary experiments, we found out that expression was 2- to 3-fold higher in High Five cells than in Sf9 cells, and expression reached a plateau after 96 h when the insect cells were infected at an MOI of 5 (data not shown). The expression of human IgG molecules was confirmed by Western blotting with anti human IgG + IgM (H + L) antibody (Jackson ImmunoResearch Laboratories Inc., West Grove, PA). Expressed proteins were purified by HiTrap Protein A columns (GE Healthcare UK Ltd.) and analyzed by SDS–PAGE under reducing and nonreducing conditions. The yield of human IgG expressed using this system was 1–5 mg/1-liter culture. SDS–PAGE analysis of the expressed human IgG showed two bands corresponding to H and L chains under reducing conditions and a single band corresponding to IgG under nonreducing conditions (Fig. 3A), suggesting that the molecules have a correct conformation. CBB staining also showed that we obtained pure human IgG after one-step purification using a protein A column.

To examine cell surface-specific reactivity, we incubated IgG27 with A24-positive B-LCL cells pulsed with Nef138-10 peptides and observed the stained cells under microscopy. The staining procedure was identical to the procedure used for flow cytometry, except that the antibody dilution buffer was FCS instead of NRS. Stained cells were mounted on Teflon Printed eight-well chamber glass slides (Erie Scientific Company, Portsmouth, NH) and observed with an Eclipse E600 microscopy system (Nikon Corporation, Tokyo, Japan). As shown in Fig. 3B (right panel), HLA-A, HLA-B, and HLA-C molecules were expressed with approximately equal frequency on the cells in the assay. Fluorescence signals appeared as dots on the cells pulsed with the Nef138-10 peptide (Fig. 3B). By contrast, cells pulsed with Env584-11 showed no fluorescence. These data suggest that the reconstituted human IgG was specific for Nef138-10/A24 on the cell surface.

We further characterized reconstituted human IgGs. ELISA analysis showed that clones IgG3 and IgG27 bound specifically to Nef138-10/A24 in a dose-dependent manner but not to Env584-11/A24 or BSA (Fig. 4). At a lower concentration clone IgG27 showed higher affinity than IgG3, consistent with staining results seen earlier with the corresponding scFvs.

FIG. 2. Flow cytometric analysis of scFvs for their binding specificity on cells pulsed with peptides. A24-positive B-LCL cells (HLA-A24, A26, B7, B52, CW7) were pulsed with 10 μM of A24-restricted epitope peptides; the Nef138-10 (RYPLTFGWCF), Env584-11 (RYLRDQQLLGI), Gag28-9 (KYKLKHIVW), and CMV pp65-328 (QYDPVAALF) were stained with each scFv clone. These cells were then stained with a biotinylated polyclonal rabbit anti-c-Myc-tag antibody (Santa Cruz Biotechnology Inc.), and finally with a PE-conjugated streptavidin. We also stained the cells with a PE-conjugated anti-HLA-ABC antibody (W6/32) to analyze the expression of HLA-ABC molecules on the cell surface. The shaded histograms show specific staining with each scFv clone whereas open histograms show background staining with a rabbit anti-c-Myc-tag antibody and a PE-conjugated streptavidin. The ordinate indicates the relative cell number and the horizontal axis indicates fluorescence intensity in a log scale.

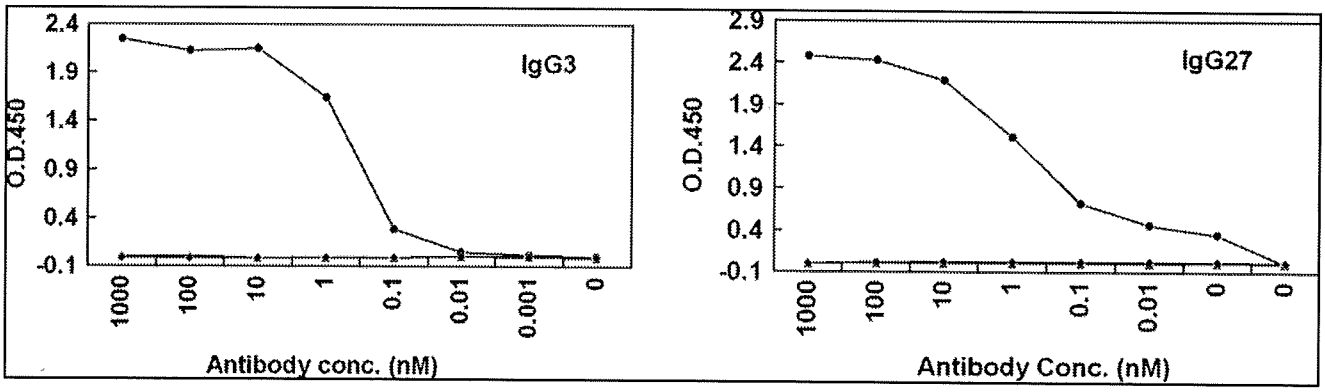

FIG. 4. Analysis of the molecular interaction of the reconstituted human IgG by ELISA. The binding specificity was analyzed by ELISA with antihuman IgG antibody (SIGMA). The bindings to Nef138-10/A24 (circle), Env584-11/A24 (triangle), and BSA(diamond) are shown. The ordinate indicates the optical density value at OD_{450}. The IgG concentration is shown below the horizontal line.

Therefore, we concluded that we had reconstituted intact human IgG molecules with the same high degree of specificity as the parental scFvs.

We also analyzed antigen–antibody interactions by surface plasmon resonance using BIAcore 1000 (GE Healthcare UK Ltd.). The analysis of the interaction between antigens and antibodies was done at 25°C under a flow rate of 20 μl/min. HBS-EP (10 mM HEPES, 150 mM NaCl, 3 mM EDTA, 0.05% Tween 20; pH 7.4) buffer was used in all experiments. The antihuman IgG Fc region antibodies were immobilized about 3700 resonance units (RU) on a research grade CM5 sensor chip (GE Healthcare UK Ltd.) by standard amine coupling. The IgG molecules were flowed on the chip and captured about 1200 RU. Nef138-10/A24 were purified further on a Mono Q column for the analysis of antigen–antibody interaction by BIAcore. Nef138-10/A24s were diluted in HBS-EP buffer containing NSB Reducer (GE Healthcare UK Ltd.) and injected for 3 min. The chip was regenerated by injecting 10 mM glycine-HCl (pH 1.5). The human IgG captured cell was used as the reference cell. Data were collected at five different concentrations of Nef138-10/A24 and analyzed by BIAevaluation 3.0 software (GE Healthcare UK Ltd.). The binding and dissociation constants were determined using data from five different concentrations (Fig. 5A). The dissociation constants of IgG3 and IgG27 were approximately 23 μM and 20 μM, respectively (Fig. 5B). The dissociation constants of the IgG3 and IgG27 clones were in the expected range for TCR interactions, but were too low for antibody interactions.[26,27] IgG27 stained Nef138-10/A24 specifically on the surface of peptide-pulsed cells. We also tried to stain the cells with expression of whole Nef protein using Sendai virus vector but could not stain endogenously expressed HIV-1 Nef CTL epitope.

The low expression of the endogenously expressed CTL epitope and the low binding affinity of the antibodies might explain the inability to detect endogenously expressed pMHCs. We speculate that clones IgG3 and IgG27 could have originated from lower-affinity IgM clones in our pooled scFv library.

In this study, we successfully isolated scFvs directed against an HIV-1-specific pMHC, Nef138-10/A24, using a panning procedure with magnetic beads to select the specific antibodies from phage display libraries. Also, we successfully reconstituted the human IgGs directed against the HIV-1 Nef138-10 CTL epitope loaded on an HLA-A24 molecule using the baculovirus expression system. All the clones that reconstituted using this system kept the same specificity of parental scFvs and were easily obtained at a high amount and purity after one-step purification. These systems will provide us with a rapid generation of monoclonal antibodies that is difficult to generate using conventional hybridoma technology. Ours is the first report to describe the generation of

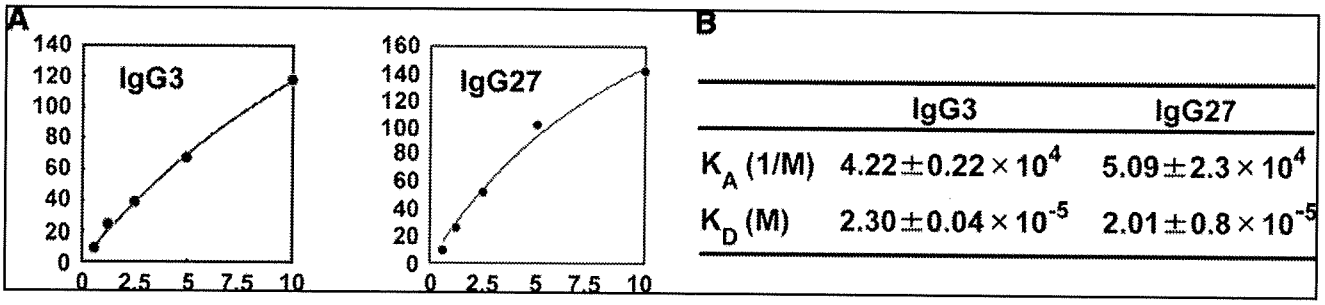

FIG. 5. Analysis of the antigen–antibody interaction using Biacore. The antibody–antigen interactions were analyzed by surface plasmon resonance. (**A**) The IgG molecules were captured on an antihuman IgG immobilized CM5 chip and Nef138-10/A24 was flowed on the chip at five different concentrations. (**B**) The data were collected and analyzed by BIAevaluation. The binding (K_a) and dissociation (K_d) constants of each IgG clone are shown in the panel.

monoclonal antibodies bound specifically to an immunodominant HIV-1 CTL epitope loaded on an HLA class I molecule. We were able to show that this particular CTL epitope had a B cell epitope. Efforts to isolate antibodies with higher affinities would be warranted. The escape phenotype associated with this particular CTL epitope may result either from structural differences of pMHCs, from aberrant processing of the mutant epitope, or from decreased numbers of pMHCs on the cell surface. To address these questions, further studies are underway using these monoclonal antibodies and some other techniques.

Acknowledgments

This work was supported in part by the Program of Founding Research Centers for Emerging and Reemerging Infectious Diseases of the Ministry of Education, Culture, Sports, Science and Technology (MEXT); Strategic Cooperation to Control Emerging and Reemerging Infections funded by the Special Coordination Funds for Promoting Science and Technology of MEXT; Grants for Research on HIV/AIDS and Research on Publicly Essential Drugs and Medical Devices from the Ministry of Health, Labor, and Welfare of Japan; and Grant-in-Aid for Scientific Research (B) from the Japan Society for the Promotion of Science (JSPS). Data were previously presented at the 4th IAS Conference on HIV Pathogenesis, Treatment and Prevention in Sydney, Australia, July 22–25, 2007 and published as an abstract under the title "Generation of monoclonal antibodies cross-reactive for the wild type and an escape mutant of an immunodominant CTL epitope."

Disclosure Statement

No competing financial interests exist.

References

1. Walker BD and Burton DR: Toward an AIDS vaccine. Science 2008;320:760–764.
2. Hedrick SM, Cohen DI, Nielsen EA, and Davis MM: Isolation of cDNA clones encoding T cell-specific membrane-associated proteins. Nature 1984;308:149–153.
3. Yanagi Y, Yoshikai Y, Leggett K, Clark SP, Aleksander I, and Mak TW: A human T cell-specific cDNA clone encodes a protein having extensive homology to immunoglobulin chains. Nature 1984;308:145–149.
4. Zinkernagel RM and Doherty PC: Restriction of *in vitro* T cell-mediated cytotoxicity in lymphocytic choriomeningitis within a syngeneic or semiallogeneic system. Nature 1974; 248:701–702.
5. Bjorkman PJ, Saper MA, Samraoui B, Bennett WS, Strominger JL, and Wiley DC: The foreign antigen binding site and T cell recognition regions of class I histocompatibility antigens. Nature 1987;329:512–518.
6. Bjorkman PJ, Saper MA, Samraoui B, Bennett WS, Strominger JL, and Wiley DC: Structure of the human class I histocompatibility antigen, HLA-A2. Nature 1987;329:506–512.
7. McMichael AJ and Rowland-Jones SL: Cellular immune responses to HIV. Nature 2001;410:980–987.
8. Schwartz O, Marechal V, Le Gall S, Lemonnier F, and Heard JM: Endocytosis of major histocompatibility complex class I molecules is induced by the HIV-1 Nef protein. Nat Med 1996;2:338–342.
9. Kelleher AD, Long C, Holmes EC, *et al.*: Clustered mutations in HIV-1 gag are consistently required for escape from HLA-B27-restricted cytotoxic T lymphocyte responses. J Exp Med 2001;193:375–386.
10. Klenerman P, Rowland-Jones S, McAdam S, *et al.*: Cytotoxic T-cell activity antagonized by naturally occurring HIV-1 Gag variants. Nature 1994;369:403–407.
11. Furutsuki T, Hosoya N, Kawana-Tachikawa A, *et al.*: Frequent transmission of cytotoxic-T-lymphocyte escape mutants of human immunodeficiency virus type 1 in the highly HLA-A24-positive Japanese population. J Virol 2004;78: 8437–8445.
12. Altman JD, Moss PA, Goulder PJ, *et al.*: Phenotypic analysis of antigen-specific T lymphocytes. Science 1996;274:94–96.
13. Lucchiari-Hartz M, van Endert PM, Lauvau G, *et al.*: Cytotoxic T lymphocyte epitopes of HIV-1 Nef: Generation of multiple definitive major histocompatibility complex class I ligands by proteasomes. J Exp Med 2000;191:239–252.
14. Tsomides TJ, Aldovini A, Johnson RP, Walker BD, Young RA, and Eisen HN: Naturally processed viral peptides recognized by cytotoxic T lymphocytes on cells chronically infected by human immunodeficiency virus type 1. J Exp Med 1994;180:1283–1293.
15. Polakova K, Plaksin D, Chung DH, Belyakov IM, Berzofsky JA, and Margulies DH: Antibodies directed against the MHC-I molecule H-2Dd complexed with an antigenic peptide: Similarities to a T cell receptor with the same specificity. J Immunol 2000;165:5703–5712.
16. Porgador A, Yewdell JW, Deng Y, Bennink JR, and Germain RN: Localization, quantitation, and in situ detection of specific peptide-MHC class I complexes using a monoclonal antibody. Immunity 1997;6:715–726.
17. Denkberg G, Cohen CJ, Lev A, Chames P, Hoogenboom HR, and Reiter Y: Direct visualization of distinct T cell epitopes derived from a melanoma tumor-associated antigen by using human recombinant antibodies with MHC-restricted T cell receptor-like specificity. Proc Natl Acad Sci USA 2002; 99:9421–9426.
18. Lev A, Denkberg G, Cohen CJ, *et al.*: Isolation and characterization of human recombinant antibodies endowed with the antigen-specific, major histocompatibility complex-restricted specificity of T cells directed toward the widely expressed tumor T-cell epitopes of the telomerase catalytic subunit. Cancer Res 2002;62:3184–3194.
19. Hashiguchi S, Nakashima T, Nitani A, *et al.*: Human Fc epsilon RIalpha-specific human single-chain Fv (scFv) antibody with antagonistic activity toward IgE/Fc epsilon RIalpha-binding. J Biochem (Tokyo) 2003;133:43–49.
20. Clackson T, Hoogenboom HR, Griffiths AD, and Winter G: Making antibody fragments using phage display libraries. Nature 1991;352:624–628.
21. McCafferty J, Griffiths AD, Winter G and Chiswell DJ: Phage antibodies: Filamentous phage displaying antibody variable domains. Nature 1990;348:552–554.
22. Biddison WE, Turner RV, Gagnon SJ, Lev A, Cohen CJ, and Reiter Y: Tax and M1 peptide/HLA-A2-specific Fabs and T cell receptors recognize nonidentical structural features on peptide/HLA-A2 complexes. J Immunol 2003;171:3064–3074.
23. Chames P, Hufton SE, Coulie PG, Uchanska-Ziegler B, and Hoogenboom HR: Direct selection of a human antibody fragment directed against the tumor T-cell epitope HLA-A1-MAGE-A1 from a nonimmunized phage-Fab library. Proc Natl Acad Sci USA 2000;97:7969–7974.

24. Cohen CJ, Hoffmann N, Farago M, Hoogenboom HR, Eisenbach L, and Reiter Y: Direct detection and quantitation of a distinct T-cell epitope derived from tumor-specific epithelial cell-associated mucin using human recombinant antibodies endowed with the antigen-specific, major histocompatibility complex-restricted specificity of T cells. Cancer Res 2002;62:5835–5844.
25. Kawana-Tachikawa A, Tomizawa M, Nunoya J, *et al.*: An efficient and versatile mammalian viral vector system for major histocompatibility complex class I/peptide complexes. J Virol 2002;76:11982–11988.
26. Sakaguchi N, Kimura T, Matsushita S, *et al.*: Generation of high-affinity antibody against T cell-dependent antigen in the Ganp gene-transgenic mouse. J Immunol 2005;174:4485–4494.
27. van der Merwe PA and Davis SJ: Molecular interactions mediating T cell antigen recognition. Annu Rev Immunol 2003;21:659–684.

Address correspondence to:
Aikichi Iwamoto
4-6-1 Shirokanedai
Minato-ku
Tokyo 108-8639, Japan

E-mail: aikichi@ims.u-tokyo.ac.jp

Journal of Virological Methods 161 (2009) 216–222

Contents lists available at ScienceDirect

Journal of Virological Methods

journal homepage: www.elsevier.com/locate/jviromet

Monitoring of HIV-1 envelope-mediated membrane fusion using modified split green fluorescent proteins

Jianqi Wang[a], Naoyuki Kondo[a,b], Yufei Long[a], Aikichi Iwamoto[b,c], Zene Matsuda[a,b,*]

[a] China-Japan Joint Laboratory of Structural Virology and Immunology, Institute of Biophysics, Chinese Academy of Sciences, 15 Datun Road, Chaoyang District, Beijing 100101, China
[b] Research Center for Asian Infectious Diseases, Institute of Medical Science, the University of Tokyo, 4-6-1, Shirokanedai Minato-ku, Tokyo 108-8639, Japan
[c] Division of Infectious Diseases, Advanced Clinical Research Center, Institute of Medical Science, the University of Tokyo, 4-6-1, Shirokanedai Minato-ku, Tokyo 108-8639, Japan

Article history:
Received 9 February 2009
Received in revised form 11 June 2009
Accepted 16 June 2009
Available online 25 June 2009

Keywords:
Split protein
GFP
HIV-1
Membrane fusion
Envelope protein
Phenotyping method

ABSTRACT

A simple, cell-based, membrane fusion assay system that uses split green fluorescent proteins (spGFPs) as an indicator was developed. The attachment of the pleckstrin homology (PH) domain to the N-termini of each spGFP not only localized the reporter signal to the plasma membrane but also helped the stable expression of the smaller spGFP of seventeen amino acid residues. It was shown that this system allowed real-time monitoring of membrane fusion by HIV-1 envelope protein (Env) without the addition of external substrates. This method can be adapted to the analyses of other viral membrane fusion.

1. Introduction

Membrane fusion is the prerequisite event that allows enveloped viruses, some of which are linked to emerging infectious diseases such as avian influenza, severe acute respiratory syndrome, and acquired immunodeficiency syndrome (AIDS), to enter their host cells. Among these emerging diseases, AIDS has become a global threat to human health. The discovery of a membrane fusion inhibitor has made HIV-1 Env an important target for anti-HIV-1 chemotherapy (Chan et al., 1997; Eckert and Kim, 2001; Este and Telenti, 2007; Poveda et al., 2005; Weissenhorn et al., 1997). Recently, a new class of inhibitor that blocks the interaction between Env and its co-receptor, CCR5, has been developed (Santoro et al., 2004). A simple phenotyping method of Env-mediated membrane fusion will facilitate progress in the development of new inhibitors or in the evaluation of drug-resistant mutants (Olson and Maddon, 2003).

A phenotyping method of HIV-1 Env requires a system that generates a measurable signal upon membrane fusion either in a cell–cell or virus–cell system. The methods described employ materials, such as visible dyes, transcription factors, and self-complementing enzyme fragments, that produce a signal when they transfer from one compartment to another via membrane fusion (Barbeau et al., 1998; Blumenthal et al., 2002; Feng et al., 1996; Furuta et al., 2006; Holland et al., 2004; Huerta et al., 2002; Jun and Wickner, 2007; Lin et al., 2005, 2003; Monck and Fernandez, 1992; Sakamoto et al., 2003).

The development of a versatile, cell-based membrane fusion assay system is described in this report. The system employs a modified green fluorescent protein (GFP), split GFP (spGFP), which has been engineered to have the capacity for self-assembly (Cabantous et al., 2005). The pleckstrin homology (PH) domain (Lemmon, 2008) was fused at the N-termini of spGFPs so as to focus the signal in the membrane regions. These spGFPs become fluorescent only when they have reassociated with each other (Cabantous et al., 2005) during the membrane fusion. Unlike an enzyme-based assay, this spGFP system allows real-time monitoring of the membrane fusion process without any additional substrates.

2. Materials and methods

2.1. Construction of expression vectors

The PH domain based on human phospholipase Cδ was synthesized by assembling 10 oligonucleotides, each containing 79 nucleotides. The oligonucleotides were combined and assembled

Abbreviations: AIDS, acquired immunodeficiency syndrome; GFP, green fluorescent protein; spGFP, split green fluorescent protein; PH, pleckstrin homology; DMEM, Dulbecco's modified Eagle's medium; MSD, membrane-spanning domain.

* Corresponding author at: Research Center for Asian Infectious Diseases, Institute of Medical Science, the University of Tokyo, 4-6-1 Shirokanedai, Minato-ku, Tokyo 109-8639, Japan. Tel.: +81 3 6409 2204; fax: +81 3 6409 2008.
E-mail address: zmatsuda@ims.u-tokyo.ac.jp (Z. Matsuda).

0166-0934/$ – see front matter © 2009 Elsevier B.V. All rights reserved.
doi:10.1016/j.jviromet.2009.06.017

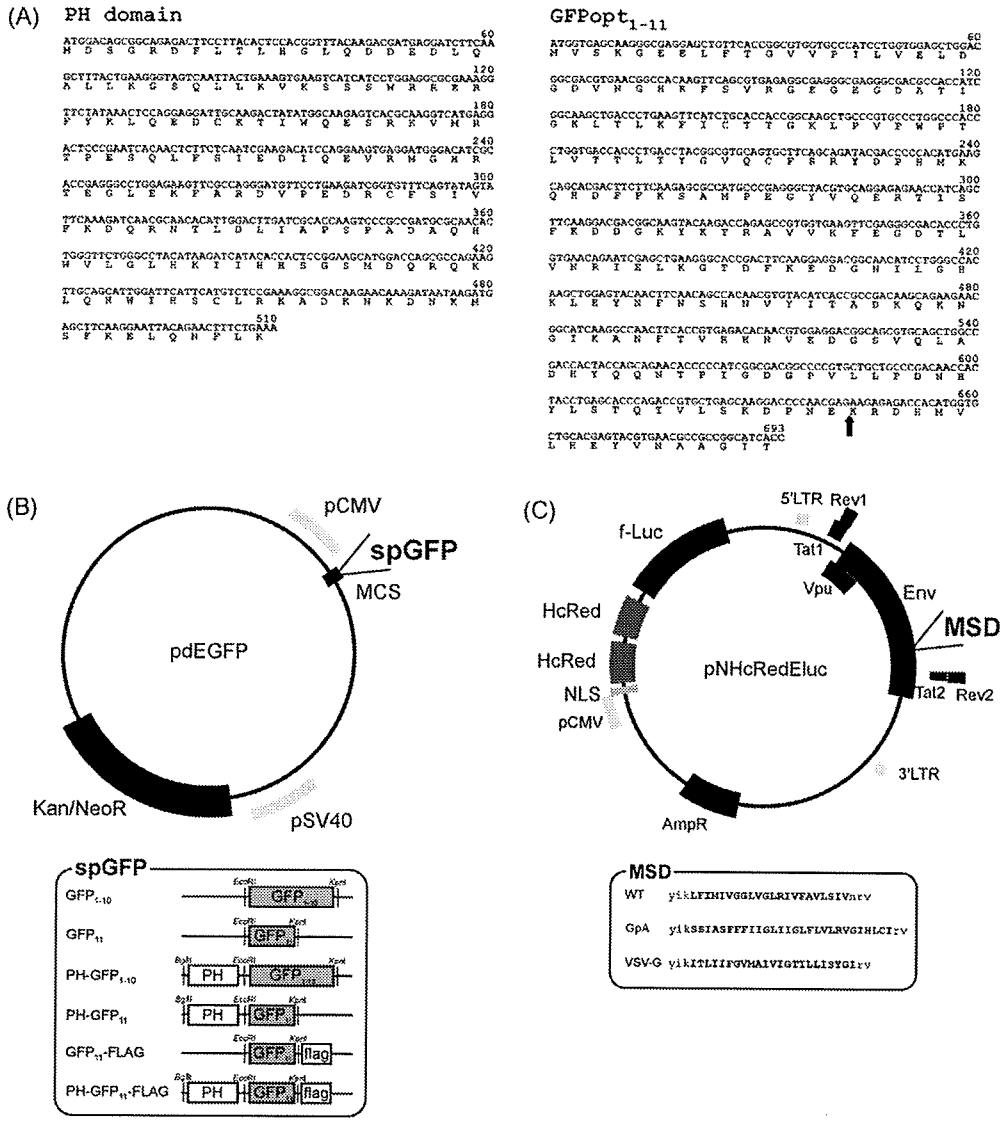

Fig. 1. Engineered proteins and expression vectors. (A) The amino acid and nucleotide sequences of PH domain and $GFPopt_{1-11}$ were shown. The amino acid residue was shown using the single-letter abbreviations. The split point between GFP_{1-10} and GFP_{11} is indicated by the arrow in $GFPopt_{1-11}$. (B) (upper panel) The expression vector for spGFPs. MCS: multiple cloning site; spGFP: the insertion point of spGFP; *Kan/NeoR*: kanamycin/neomycin resistance gene. (Lower panel) The different spGFPs. PH: pleckstrin homology domain. The restriction sites that were used are indicated. (C) (upper panel) The HIV-1 envelope expression vector, pNHcRedEluc. pCMV: human cytomegalovirus promoter, NLS: nuclear-localization signal, HcRed: a far-red fluorescent protein isolated from *Heteractis crispa*, f-Luc: firefly luciferase, MSD: membrane-spanning domain, *AmpR*: ampicillin resistance gene. (Lower panel) Primary structures of the MSDs used. WT: wild type, GpA: glycophorin A, VSV-G: vesicular stomatitis virus G protein. The predicted MSD regions are capitalized.

by PCR (94 °C for 30 s, 50 °C for 30 s, 72 °C for 40 s for 30 cycles). Similarly, 30 oligonucleotides, which overlapped each other with 18 bases at the both ends, were used to assemble the optimized GFP gene, named $GFPopt_{1-11}$. The primary sequences of the PH domain and $GFPopt_{1-11}$ are shown in Fig. 1A. Both amplicons were cloned and sequenced in pCR4Blunt-TOPO (Invitrogen, Carlsbad, USA). $GFPopt_{1-11}$ was split into GFP_{1-10} (1–642 base pairs) and GFP_{11} (643–696 base pairs), at a point between the 10th and 11th β-sheets of the GFP. The subscripts 1–10 and 11 reflect this location. The PH-GFP_{1-10} and PH-GFP_{11} genes were generated by combining the PH domain gene with the spGFP genes. These genes were then cloned to pdEGFP, which was constructed by deleting the EGFP gene in pEGFP-N2 (BD Biosciences Clontech, Palo Alto, USA) (Fig. 1B). The expression vector for each protein was named by adding pd in front of the target protein, such as pdPH-GFP_{1-10}.

The FLAG tag sequence was added to the 3′-termini of the spGFP genes by using a 3′-primer that included the FLAG tag sequence during PCR. A new HIV-1 Env-expression vector called pNHcRedEluc, a derivative of pElucEnv (Miyauchi et al., 2005), was constructed by replacing the gene for EGFP with that of a tandem red fluorescent protein; HcRed (Evrogen, Moscow, Russia). This was preceded by a nuclear-localizing signal (Fig. 1C). Thus the nuclei of transfected cells became red. The transfection efficiency could then be measured by firefly luciferase activity. The pNHcRedEluc△NB vector in which most of the env gene had been deleted was prepared as a negative control.

2.2. Cell cultures and transfection

The 293FT (Invitrogen, Carlsbad, USA) and 293CD4 (Miyauchi et al., 2005) cells were maintained in Dulbecco's modified Eagle's medium (DMEM, Sigma, St. Louis, USA) supplemented with 10% fetal bovine serum (Hyclone, Logan, USA). The 293FT cells were cultured with 500 μg/ml of Geneticin (Gibco, Grand Island, USA),

as recommended by the manufacturer. Transient transfection was accomplished using Fugene HD (Roche, Indianapolis, USA). Stable cell lines expressing PH-GFP$_{1-10}$ were established after transfecting 293CD4 cells with pdPH-GFP$_{1-10}$ by electroporation (Biorad GenePulsar, Hercules, USA). Transfected cells were selected with 700 μg/ml of Geneticin in DMEM.

2.3. Fusion assay

The spGFP-mediated fusion assay was performed as follows. The expression vectors pNHcRedEluc and pdPH-GFP$_{11}$ were transfected into 293FT cells. The transfected 293FT cells were overlaid with 293CD4 cells which were transfected transiently or permanently with vector pdPH-GFP$_{1-10}$. In the case of transient transfection, the mixing of cells was started at 42 h after transfection. Fusion was monitored in real-time using an IN Cell Analyzer 1000 (GE Healthcare, Uppsala, Sweden) or was observed using a confocal microscope (Olympus FluoView FV1000, Tokyo, Japan) that examined fixed cells (4% paraformaldehyde) at designated time points.

The fusion assay using the mixing of the two different fluorescent proteins expressed in the Env(+)- and receptor(+) cells, respectively as an indicator was carried out as follows. The pElucEnv (Miyauchi et al., 2005) was transfected into 293FT cells to make Env(+) cells. Because pElucEnv expressed both the HIV-1 Env and GFP proteins, this generated "green" Env(+) cells. Meanwhile the expression vector for DsRed (Clontech/Takara, Otsu, Japan) was transfected into 293CD4 cells to generate "red" receptor(+) cells. These two types of cells were co-cultured and the extent of the fusion was monitored by the redistribution of the green and red signals by microscopy.

The inhibitor C34 was used to show the specificity of the new fusion assay. According to the previous study (Kliger et al., 2001), two different concentrations, 12 nM and 150 nM in a final concentration, of the peptide inhibitor, C34, was added at the beginning of the co-culture. The IC50 value of the C34 peptide was about 12 nM and more than 90% inhibition was observed with the concentration of 150 nM (Kliger et al., 2001). The cells were fixed and examined after 2.5 h of co-culture and analyzed as described above.

2.4. Protein analysis

Sample preparation and immunoblotting were done as described previously (Miyauchi et al., 2005). Anti-FLAG antibody (Sigma, Saint Louis, USA) and anti-GFP antibody (Santa Cruz Biotechnology, Santa Cruz, USA) were used as primary antibodies for the analysis of GFP$_{11}$ and GFP$_{1-10}$, respectively. Chemiluminescence signals were detected using an LAS-3000Lite (Fujifilm, Tokyo, Japan).

2.5. Immunofluorescence assay

Transfected cells were fixed in an acetone:methanol solution (1:1) for 15 min at room temperature and stained with an anti-FLAG antibody (3 μg/ml) for 40 min at 30 °C. A secondary antibody, labeled with Alexa Fluor 555 (Invitrogen, Carlsbad, USA), was used. The fluorescent signal was observed using a confocal microscope (Olympus FluoView FV1000, Tokyo, Japan).

3. Results

3.1. Expression of modified spGFPs

3.1.1. Immunoblotting analysis

The expression vectors containing different spGFPs shown in Fig. 1B were transfected into the cells and the expressed proteins were then analyzed by immunoblotting. When probed with an anti-GFP antibody, GFP$_{1-10}$ and PH-GFP$_{1-10}$ were detected as approximately 25 kDa and 40 kDa bands, respectively (Fig. 2A). The observed molecular weights were consistent with those expected from the amino acid sequences. The cells transfected with pEGFP-N2 (BD Biosciences Clontech) were included as a positive control (Fig. 2A, EGFP lane). As for GFP$_{11}$, an anti-GFP antibody failed to detect any band (data not shown). A FLAG tag was added to GFP$_{11}$ with and without the PH domain because this failure could have been caused by the absence of anti-GFP's epitope in the seventeen-amino-acid-long GFP$_{11}$ portion. When probed with an anti-FLAG antibody, a band of 22 kDa was detected for PH-GFP$_{11}$-FLAG but not for GFP$_{11}$-FLAG (Fig. 2B). This result suggested that GFP$_{11}$, as only a seventeen-amino-acid-long peptide, was unstable without the PH domain.

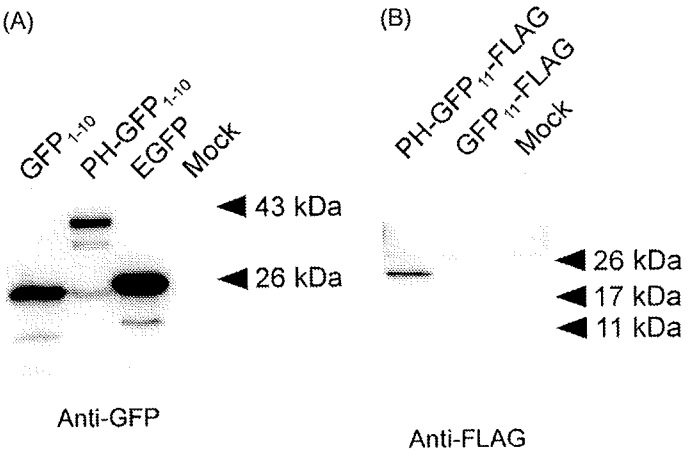

Fig. 2. The spGFPs expressed in the transfected cells. (A) Immunoblotting analysis of 293CD4 cells transfected with GFP$_{1-10}$ and PH-GFP$_{1-10}$ expression vectors and probed with an anti-GFP antibody. Cells transfected with pEGFP-N2 (BD Biosciences Clontech) were included as a positive control (EGFP lane). (B) The proteins expressed in 293FT cells transfected with the GFP$_{11}$-FLAG or the PH-GFP$_{11}$-FLAG expression vectors were probed with an anti-FLAG monoclonal antibody. Mock: the mock transfected cells.

3.1.2. Immunofluorescence analysis

Immunofluorescence analysis was used to examine the intracellular localization of the spGFPs. The GFP$_{1-10}$ distributed throughout the cell, but with the PH domain attached, the PH-GFP$_{1-10}$ localized to the periphery of the transfected cells (Fig. 3A). The expression of FLAG-tagged GFP$_{11}$ (Fig. 3B, top) was not detected. This finding is consistent with the results of immunoblotting (Fig. 2B). However, FLAG-tagged PH-GFP$_{11}$ was detectable at the cell periphery (Fig. 3B, middle). Without the FLAG tag, PH-GFP$_{11}$ showed no signal with anti-FLAG antibody (Fig. 3B, bottom).

3.2. Recovery of GFP function by reassociation of spGFPs

Next, pairs of the spGFPs were co-transfected into 293FT cells and their outcome was examined (Fig. 3C). Consistent with the data shown in Fig. 2, PH-GFP$_{11}$, but not free GFP$_{11}$, was able to generate a green signal (Fig. 3C). When PH-GFP$_{11}$ was co-transfected with GFP$_{1-10}$, a homogenous green signal was observed. This data suggests that the reassociation of two split GFPs could take place before they are localized to the plasma membrane. With the pair of PH-GFP$_{1-10}$ and PH-GFP$_{11}$, most of the green signal was detected in the rim of the co-transfected cells (Fig. 3C). As expected, neither the spGFPs nor the PH-spGFPs alone showed any fluorescence (Fig. 3D).

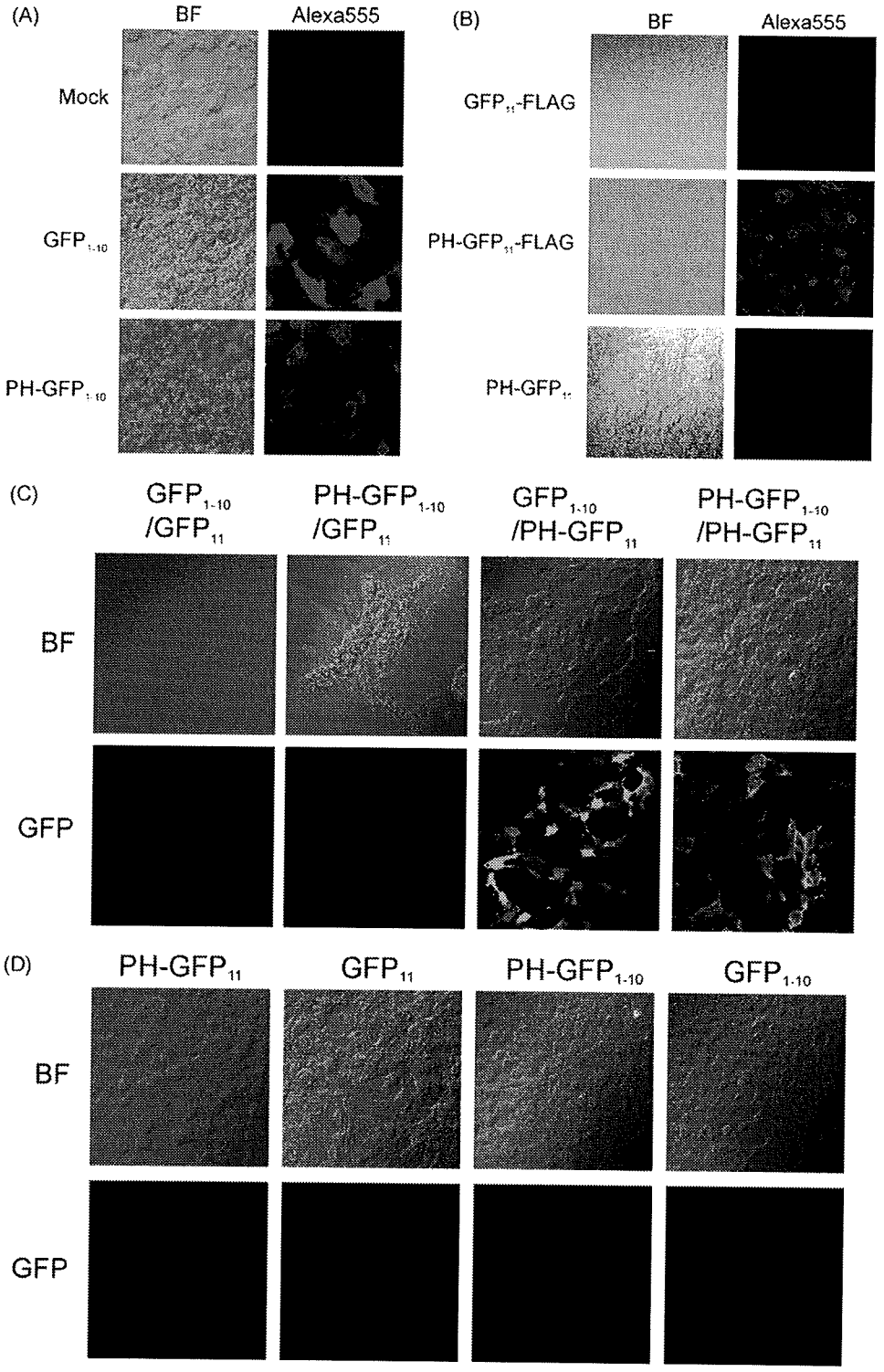

Fig. 3. Intracellular localization of spGFPs expressed with pdExpression vectors. (A) Immunofluorescence assay of GFP_{1-10} or PH-GFP_{1-10}-transfected cells using an anti-GFP antibody. Mock: mock transfected cells; BF: bright field view; Alexa555: the Alexa555-derived signal. (B) Immunofluorescence assay of GFP_{11}-FLAG, PH-GFP_{11}-FLAG, and PH-GFP_{11}-transfected cells using anti-FLAG antibody. The abbreviations used are the same as for (A). (C) Co-transfection of PH-GFP_{1-10} with PH-GFP_{11} and GFP_{11} and of GFP_{1-10} with PH-GFP_{11} and GFP_{11}. (D) Single transfection of different spGFPs. BF: bright field view; GFP: the GFP signal.

3.3. Membrane fusion assay using spGFPs

3.3.1. Analysis of the wild type HIV-1 Env-mediated fusion

PH-spGFPs was used for the analysis of membrane fusion induced by HIV-1 Env. For this, the 293FT cells were transfected with pNHcRedEluc and pdPH-GFP_{11} and then co-cultured with the 293CD4 cells that were stably expressing PH-GFP_{1-10}. The green signal was observed at the plasma membrane surrounding several red nuclei (Fig. 4A). The red nuclei were derived from the 293FT cells expressing Env as pNHcRedEluc expressed the nuclear-localizing HcRed proteins. The unique localization of green signal in the membrane region made it easy to differentiate the real signal from the non-specific autofluorescence background. Furthermore, the non-envelope-mediated spontaneous fusions, if they occurred, could be

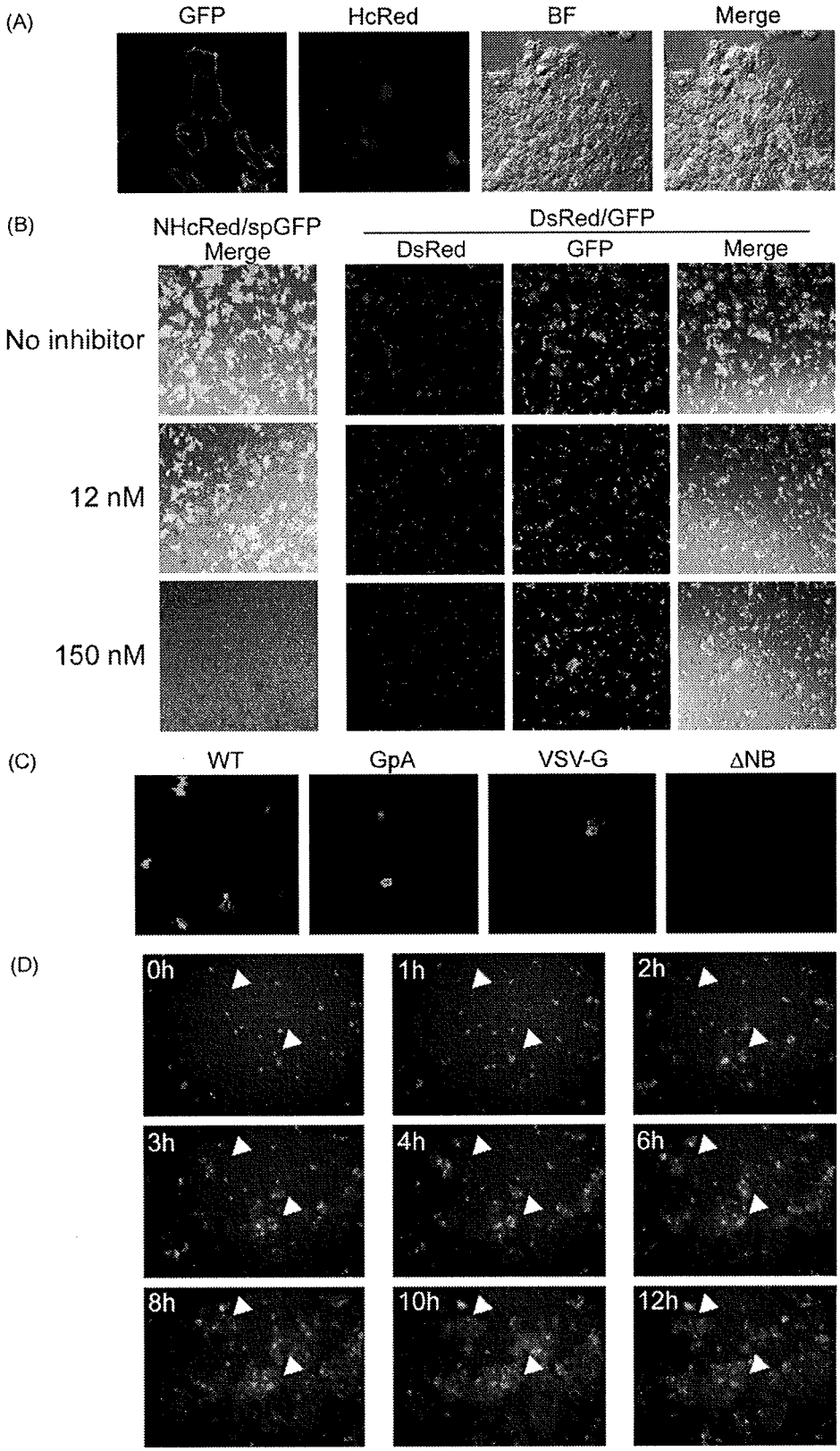

Fig. 4. Generation of the green fluorescent signal upon membrane fusion. Cell fusion between envelope- and receptor-expressing cells that harbor respective spGFP expression vectors were observed using a confocal microscope and IN Cell Analyzer. The HcRed signal was generated from the cells transfected with the expression vector for envelope and HcRed genes (Fig. 1C). (A) Detailed image of the localization of spGFPs and HcRed. BF indicates bright field; GFP: the green fluorescence signal; Merge: the merged images of GFP, HcRed, and BF. (B) The effect of the specific inhibitor and comparison with the fluorescent proteins-mixing assay. The specific inhibitor of the HIV-1 Env-mediated membrane fusion, C34, was used in the spGFP assay (left) and the conventional fluorescent protein-mixing assay (right). The final concentration of the inhibitor was indicated in nM. In the fluorescent protein-mixing assay (right), Env(+)-293FT cells expressing GFP and the receptor(+)-293CD4 cells expressing DsRed were co-cultured. Fused cells are seen as both GFP and DsRed signal-positive cells. (C) Comparison of the frequency of membrane fusion events between wild type (WT) and its MSD mutants (GpA and VSV-G) (details are in Fig. 1C). ΔNB indicates Env-deleted pNHcRedEluc. (D) The time-course analyses. Arrowheads indicate the regions of observed GFP signal. The time after co-culture is indicated in the upper left of each image.

ruled out by the absence of red nuclei in the syncytia. This result indicates that the simultaneous use of pNHcRedEluc and spGFPs allows us to monitor membrane fusion directly without the addition of dyes or substrates.

3.3.2. Analysis of HIV-1 Env-mediated fusion using an inhibitor and Env mutants

The specificity of the spGFP assay was examined by using the known inhibitor of the HIV-1 Env-mediated membrane fusion, C34 (Seo et al., 2005). The C34 peptide is known to inhibit the formation of 6-helix bundle. Two different concentrations, 12 nM (IC50) and 150 nM (IC90) (Kliger et al., 2001), were tested in spGFP fusion assays. For a comparison, in addition to the spGFP assay, the fusion assay using the Env(+)- or receptor(+)-cells expressing GFP and DsRed, respectively was used. In the spGFP assay, the number of the GFP signal-positive cells was decreased in a dose-dependent manner (Fig. 4B, left column). In a parallel assay, the number of the fused cells indicated by the presence of the both GFP and RFP signals in the fused cells was decreased similarly (Fig. 4B, right panel). The new spGFP assay was much easier to monitor, because the green signal was only observed when the actual fusion took place. In a conventional method relying on the mixture or redistribution of the two colors was more time consuming, because each cell has to be scored for the presence of either or both colors.

The previously described fusion-inefficient mutant Env that carries the mutation in the membrane-spanning domain (MSD) (Fig. 1C, lower panel) (Miyauchi et al., 2005) was also analyzed. Consistent with previous data (Miyauchi et al., 2005), the MSD mutants showed the fusion events but less frequently, as exemplified by the lower number of cells bearing the green signal (Fig. 4C).

3.3.3. Real-time membrane fusion assay

The membrane fusion in a real-time manner using spGFP system was monitored with an IN Cell Analyzer 1000. The green signal derived from the reassociated spGFPs gradually increased in the number and intensity over the observation period (Fig. 4D). When T7 RNA polymerase transfer assay was applied (Miyauchi et al., 2005), a corresponding increase in the reading of the reporter enzyme was observed (data not shown). Using the transient transfection system, we performed several tests to determine the timing needed to detect the green signal. Sometimes the signal was detected as early as 30 min after co-culturing. A more reliable result, however, was obtained after more than 1 h co-cultivation.

4. Discussion

A cell-based assay system of membrane fusion that uses spGFP has been developed. It was found that the PH domain not only localizes the signal resulting from the spGFPs reassociated to the membrane but also aids the stable expression of GFP_{11}.

The new spGFP-mediated system is cost- and labor-efficient. First, the same living co-cultured cells can be monitored for real-time monitoring over a prolonged period (Fig. 4D). Second, the reassociated spGFPs will produce a measurable signal without any additional reagents. The dye-mediated fusion assay requires preloading of dyes before the fusion reaction (Blumenthal et al., 2002). A quantitative fusion assay using enzymes, either as pre-expressed self-complementing enzyme fragments or as induced reporter enzymes, requires the addition of enzyme substrates to monitor the processes (Cavrois et al., 2002; Holland et al., 2004; Jun and Wickner, 2007). Furthermore, if a particular substrate is membrane impermeable, continuous monitoring of the same sample is impossible because the cells have to be lysed for the assay.

Simple assay systems described in this study are suitable for high-throughput analyses. The combination of dye-transfer and fluorescence-activated cell sorting can achieve this (Huerta et al., 2002; Lin et al., 2003). However, the system reported in this study is much simpler than these methods because it generates the detectable signal only when fusion actually occurs. In the dye-transfer assay or similar "color"-mixing assay shown in Fig. 4B, one has to discriminate the simple aggregation from real fusion because the dye signals are persistent throughout the assay.

As shown in the Fig. 4C, the lower incidence of membrane fusion induced by mutant Envs was detected as visible foci with the spGFP system. If one can clone the envelope genes from clinical samples into an appropriate expression vector, this system may be useful for detecting a minor population of Env that possesses the different co-receptor usage. Such a tropism assay can be easily adapted by using CCR5/CD4+ cells together with CXCR4/CD4+ cells. Similar identification of fusion foci can be achieved if GFP is used as a reporter gene in a transcriptional factor transfer assay, such as T7 RNA polymerase or Tat (Barbeau et al., 1998; Feng et al., 1996; Lin et al., 2005; Sakamoto et al., 2003), but the need for de novo transcription/translation steps may result in a longer lag time for signal generation. Of course, membrane fusion by viruses other than HIV-1 can be monitored easily.

This spGFP-based system does not require on-going transcription/translation steps during membrane fusion. Therefore, when the tag for a different intracellular compartments is applied, the system can be used to detect communication between two compartments in the cell, such as that which occurs in vesicular transport. The application of the spGFP in other biological systems has been described previously (Feinberg et al., 2008).

Acknowledgements

This work was supported by a contract research fund from the Ministry of Education, Culture, Sports, Science and Technology of Japan for the Program of Founding Research Centers for Emerging and Reemerging Infectious Diseases. We thank Dr. Kunito Yoshiike for his critical reading of the manuscript. We also thank A.M. Menting, an editorial consultant, for help in the preparation of the manuscript.

References

Barbeau, B., Fortin, J.F., Genois, N., Tremblay, M.J., 1998. Modulation of human immunodeficiency virus type 1-induced syncytium formation by the conformational state of LFA-1 determined by a new luciferase-based syncytium quantitative assay. J. Virol. 72, 7125–7136.

Blumenthal, R., Gallo, S.A., Viard, M., Raviv, Y., Puri, A., 2002. Fluorescent lipid probes in the study of viral membrane fusion. Chem. Phys. Lipids 116, 39–55.

Cabantous, S., Terwilliger, T.C., Waldo, G.S., 2005. Protein tagging and detection with engineered self-assembling fragments of green fluorescent protein. Nat. Biotechnol. 23, 102–107.

Cavrois, M., De Noronha, C., Greene, W.C., 2002. A sensitive and specific enzyme-based assay detecting HIV-1 virion fusion in primary T lymphocytes. Nat. Biotechnol. 20, 1151–1154.

Chan, D.C., Fass, D., Berger, J.M., Kim, P.S., 1997. Core structure of gp41 from the HIV envelope glycoprotein. Cell 89, 263–273.

Eckert, D.M., Kim, P.S., 2001. Mechanisms of viral membrane fusion and its inhibition. Annu. Rev. Biochem. 70, 777–810.

Este, J.A., Telenti, A., 2007. HIV entry inhibitors. Lancet 370, 81–88.

Feinberg, E.H., Vanhoven, M.K., Bendesky, A., Wang, G., Fetter, R.D., Shen, K., Bargmann, C.I., 2008. GFP reconstitution across synaptic partners (GRASP) defines cell contacts and synapses in living nervous systems. Neuron 57, 353–363.

Feng, Y., Broder, C.C., Kennedy, P.E., Berger, E.A., 1996. HIV-1 entry cofactor: functional cDNA cloning of a seven-transmembrane, G protein-coupled receptor. Science 272, 872–877.

Furuta, R.A., Nishikawa, M., Fujisawa, J., 2006. Real-time analysis of human immunodeficiency virus type 1 Env-mediated membrane fusion by fluorescence resonance energy transfer. Microbes Infect. 8, 520–532.

Holland, A.U., Munk, C., Lucero, G.R., Nguyen, L.D., Landau, N.R., 2004. Alpha-complementation assay for HIV envelope glycoprotein-mediated fusion. Virology 319, 343–352.

Huerta, L., Lamoyi, E., Baez-Saldana, A., Larralde, C., 2002. Human immunodeficiency virus envelope-dependent cell–cell fusion: a quantitative fluorescence cytometric assay. Cytometry 47, 100–106.

Jun, Y., Wickner, W., 2007. Assays of vacuole fusion resolve the stages of docking, lipid mixing, and content mixing. Proc. Natl. Acad. Sci. U.S.A. 104, 13010–13015.
Kliger, Y., Gallo, S.A., Peisajovich, S.G., Munoz-Barroso, I., Avkin, S., Blumenthal, R., Shai, Y., 2001. Mode of action of an antiviral peptide from HIV-1. Inhibition at a post-lipid mixing stage. J. Biol. Chem. 276, 1391–1397.
Lemmon, M.A., 2008. Membrane recognition by phospholipid-binding domains. Nat. Rev. Mol. Cell Biol. 9, 99–111.
Lin, G., Murphy, S.L., Gaulton, G.N., Hoxie, J.A., 2005. Modification of a viral envelope glycoprotein cell–cell fusion assay by utilizing plasmid encoded bacteriophage RNA polymerase. J. Virol. Methods 128, 135–142.
Lin, X., Derdeyn, C.A., Blumenthal, R., West, J., Hunter, E., 2003. Progressive truncations C terminal to the membrane-spanning domain of simian immunodeficiency virus Env reduce fusogenicity and increase concentration dependence of Env for fusion. J. Virol. 77, 7067–7077.
Miyauchi, K., Komano, J., Yokomaku, Y., Sugiura, W., Yamamoto, N., Matsuda, Z., 2005. Role of the specific amino acid sequence of the membrane-spanning domain of human immunodeficiency virus type 1 in membrane fusion. J. Virol. 79, 4720–4729.
Monck, J.R., Fernandez, J.M., 1992. The exocytotic fusion pore. J. Cell Biol. 119, 1395–1404.
Olson, W.C., Maddon, P.J., 2003. Resistance to HIV-1 entry inhibitors. Curr. Drug Targets Infect. Disord. 3, 283–294.
Poveda, E., Briz, V., Soriano, V., 2005. Enfuvirtide, the first fusion inhibitor to treat HIV infection. AIDS Rev. 7, 139–147.
Sakamoto, T., Ushijima, H., Okitsu, S., Suzuki, E., Sakai, K., Morikawa, S., Muller, W.E., 2003. Establishment of an HIV cell–cell fusion assay by using two genetically modified HeLa cell lines and reporter gene. J. Virol. Methods 114, 159–166.
Santoro, F., Vassena, L., Lusso, P., 2004. Chemokine receptors as new molecular targets for antiviral therapy. New Microbiol. 27, 17–29.
Seo, J.K., Kim, H.K., Lee, T.Y., Hahm, K.S., Kim, K.L., Lee, M.K., 2005. Stronger anti-HIV-1 activity of C-peptide derived from HIV-1 89.6 gp41 C-terminal heptad repeated sequence. Peptides 26, 2175–2181.
Weissenhorn, W., Dessen, A., Harrison, S.C., Skehel, J.J., Wiley, D.C., 1997. Atomic structure of the ectodomain from HIV-1 gp41. Nature 387, 426–430.

doi: 10.1111/j.1744-313X.2007.00658.x

A three-base-deletion polymorphism in the upstream non-coding region of human interleukin 7 (IL-7) gene could enhance levels of IL-7 expression

H. Song,* E. E. Nakayama,* S. Likanonsakul,† C. Wasi,‡ A. Iwamoto§ & T. Shioda*

Summary

Interleukin 7 (IL-7) is a key factor in the survival, development and proliferation of B and T lymphocytes. Elevation of plasma IL-7 has been reported in several lymphopenia cases such as HIV-1 patients. After patients started to receive antiretroviral drugs and their $CD4^+$ cell counts had recovered, IL-7 in plasma decreased to normal levels. There are considerable variations in the levels of plasma IL-7 as well as the rate of $CD4^+$ T-cell restoration. Although pre-treatment plasma IL-7 levels have been shown to be prognostic for the rate of post-treatment $CD4^+$ T-cell restoration, the mechanisms responsible for the variations in plasma IL-7 and rate of $CD4^+$ T-cell restoration are still completely unknown. In the study here, we searched for genetic polymorphisms that might affect levels of IL-7 gene expression. For this purpose, we used 1658-bp PCR-amplified fragments of the IL-7 gene containing 1470 bp of the upstream non-coding region obtained from 151 Japanese and 234 Thai subjects. We found two novel human genetic polymorphisms in the upstream non-coding region of the IL-7 gene. The luciferase reporter assay demonstrated that one of those polymorphisms could increase the gene expression of IL-7. We speculate that this polymorphism, a three base ATC deletion just upstream of an out-of-frame ATG codon in the upstream non-coding region of the IL-7 gene, reduces the efficiency of translation from the upstream, out-of-frame ATG, resulting in increased translation efficiency from the authentic ATG of IL-7. Although the frequency of this allele is very low, it would be interesting to analyse this polymorphism in HIV-1-infected individuals with different rates of immune reconstitution after treatment with a highly active antiretroviral therapy.

* Department of Viral Infections, Research Institute for Microbial Diseases, Osaka University, Osaka, Japan, † Bamrasnaradura Institute, Nonthaburi, Thailand, ‡ Department of Microbiology, Faculty of Medicine Siriraj Hospital, Mahidol University, Bangkok, Thailand and § Division of Infectious Diseases, Institute of Medical Science, University of Tokyo, Tokyo, Japan

Received 4 July 2006; revised 17 October 2006; accepted 26 November 2006

Correspondence: Tatsuo Shioda, Department of Viral Infections, Research Institute for Microbial Diseases, Osaka University, 3–1 Yamada-Oka, Suita, Osaka 565-0871, Japan. Tel: +81 6 6879 8346; Fax: +81 6 6879 8347; E-mail: shioda@biken.osaka-u.ac.jp

This work was supported by grants from the Human Health Foundation, the Ministry of Education, Culture, Sports, Science, and Technology, and the Ministry of Health, Labour and Welfare, Japan.
There is no conflict of interest.
Haihan Song, E-mail: hhsong@biken.osaka-u.ac.jp
Emi E. Nakayama, E-mail: emien@biken.osaka-u.ac.jp
Sirirat Likanonsakul, E-mail: siratlik@health.moph.go.th
Chantapong Wasi, E-mail: sicws@mahidol.ac.th
Aikichi Iwamoto, E-mail: aikichi@ims.u-tokyo.ac.jp

Introduction

Human interleukin 7 (IL-7) is a cytokine produced by stromal cells of the thymus and bone marrow (Wolf & Cohen, 1992; Heufler *et al.*, 1993; Sudo *et al.*, 1993) and has the capacity to induce growth of immature B lymphocytes (Namen *et al.*, 1988). Similarly, IL-7 contributes to the development, proliferation and homeostatic maintenance of T cells (Grabstein *et al.*, 1990; Plum *et al.*, 1996; Schluns *et al.*, 2000; Fry *et al.*, 2001). Human IL-7 gene located on chromosome 8q12–13, has six exons that distributed to more than 33-Kb of genomic DNA (Lupton *et al.*, 1990; Fry & Mackall, 2002). It is known that the IL-7 gene has no canonical core promoter sequence in the 5′ upstream region (Lupton *et al.*, 1990; Oshima *et al.*, 2004). Recently, it has been reported, however, that transcription start sites of the IL-7 gene are clustered within two distinct regions that are approximately 515 bp to 600 bp and 130 bp to 217 bp upstream from the translation initiation ATG codon (Oshima *et al.*, 2004). Moreover, the region −282 to −251 upstream from the initiation ATG codon contains an interferon regulatory factor element (IRF-E) and could thus up-regulate the transcription of the IL-7 gene upon stimulation with gamma interferon (IFN-γ) in human intestinal epithelial cells (Oshima *et al.*, 2004). This study also revealed the presence of several out-of-frame ATG codons with unknown function in the upstream non-coding region of the IL-7 gene (Oshima *et al.*, 2004).

With respect to HIV-1 infection, there is a reverse correlation between $CD4^+$ T-cell numbers and IL-7 plasma levels in HIV-1-infected patients (Llano *et al.*, 2001; Beq *et al.*, 2004; Kopka *et al.*, 2005). After these patients started to receive antiretroviral drugs and their $CD4^+$ T-cell counts had recovered, the elevated IL-7 in the plasma decreased to normal levels (Llano *et al.*, 2001). Furthermore, it is well known that there are considerable variations in the levels of plasma IL-7 as well as the rate of CD4 T-cell restoration after HIV-1 patients started to

receive antiretroviral drugs, and pre-treatment plasma IL-7 levels have been shown to be prognostic for the rate of post-treatment CD4 T-cell restoration (Beq *et al.*, 2004). However, knowledge of the molecular mechanisms controlling IL-7 gene expression remains very limited, and the mechanisms responsible for the variations in plasma IL-7 levels and rate of CD4 T-cell restoration among individuals are still completely unknown.

Human genetic polymorphisms have recently been shown to affect expression of the corresponding genes and to consequently modify the clinical course of several human diseases such as HIV-1 infection (Dean *et al.*, 1996; Michael *et al.*, 1997; Kostrikis *et al.*, 1998; Liu *et al.*, 1999; Nakayama *et al.*, 2000). We aimed to know the molecular mechanisms controlling variations in IL-7 gene expression among individuals. For this purpose, we searched for genetic polymorphisms that might affect levels of IL-7 gene expression in 1658-bp PCR-amplified fragments of the IL-7 gene containing 1470 bp of the upstream non-coding region, 9 bp of the first coding exon and 179 bp of the downstream intron, although there was no previous report on human genetic polymorphisms that alter the levels of IL-7 gene expression. We found two novel human genetic polymorphisms in the upstream non-coding region of the IL-7 gene, one of which could enhance IL-7 expression probably by reducing the efficiency of translation from an upstream, out-of-frame ATG that would result in diminished efficiency of translation from the downstream initiation ATG.

Materials and methods

Genotyping of IL-7 gene

Human genomic DNA was obtained from peripheral blood mononuclear cells of 52 unrelated non-HIV-1-infected and 99 HIV-1-infected Japanese, as well as 122 non-HIV-1-infected and 112 HIV-infected Thais, who provided written informed consent. Genomic regions of 1658 nucleotides containing 1470 nucleotides of the upstream non-coding region and the first exon and part of the intron of IL-7 were amplified by using the primer pair P1: 5′-TCCCTCCTCTTCCTTGTTC-3′ and P2: 5′-GGTTCAAGTGGCTATGTGC-3′. Polymerase chain reaction (PCR) was run for 40 cycles of denaturation at 94 °C for 30 s, annealing at 53 °C for 30 s and extension at 72 °C for 2 min. Fluorescence-based automated cycle sequencing of the PCR products was then carried out by an ABI 3100 using P1, P2 (mentioned previously), P3: 5′-TGCTGCATTTGGGCTGTAGA-3′, P4: 5′-TGGTTTTTCCTGCGGTGAT-3′ and P5: 5′-GGTCTGCAGGTTCAATCT-3′ as sequencing primers.

Luciferase reporter gene assays

NheI and NcoI-tagged DNA fragments, corresponding to the sequences spanning positions −632 to +3, −632 to −67 and −297 to +3 from the initiation ATG of the IL-7 gene, were inserted into the corresponding restriction enzyme cleavage sites of the pGL3-Basic Vector in order to fuse ATGs in the IL-7 gene directly to the firefly luciferase open reading frame (Promega, Madison, WI). Constructs carrying an ATC deletion at position −29 to −27 from the initiation ATG of IL-7 were generated by PCR-based in vitro mutagenesis using P6: 5′-GGCTAGCAGACGACTTGGCATCGTCC-3′ and P8: 5′-TGGACCATGGTCTGCGGGAGGCGGGCGTAGTCATGACCGC-3′ or P7: 5′-GGCTAGCAGATTGAACCTGCAGACCA-3′ and P8 (mentioned previously) as the respective primer pairs for the −632 to +3 or −297 to +3 upstream region of the IL-7 gene with ATC deletion. All constructs were verified for sequence authenticity. Four micrograms of the resultant constructs was transfected with DMRIE-C (Gibco/BRL, Gaithersburg, MD) into Jurkat ($CD4^+$ T-lymphocyte cell line) and U937 cells (monocytic cell line). Transfection efficiency was normalized by cotransfection with 0.2 μg of pRL-CMV vector, which expresses *Renilla* luciferase under the control of the cytomegalovirus immediate early promoter. When necessary, INF-γ (Peprotech, Rocky Hill, NJ) was added to the transfected cell culture at a final concentration of 50 ng mL^{-1} 5 h after transfection. The cells were harvested 40 h after transfection, and firefly and *Renilla* luciferase activities were determined according to the manufacturer's instructions (Dual-Luciferase Reporter Assay System, Promega) with a Luminometer Centro LB960 (Berthold, Bad Wildbad, Germany). Relative luciferase expression (fold increase) was calculated with the following equation: fold increase = (firefly luciferase activity of upstream region of IL-7 gene construct/*Renilla* luciferase activity) / (firefly luciferase activity of promoterless vector pGL3-Basic/*Renilla* luiferase activity).

Statistical analysis

The unpaired *t*-test was used.

Results

Polymorphisms in the upstream non-coding region of the IL-7 gene

We sequenced a 1658-bp PCR-amplified fragment of the IL-7 gene containing 1470 bp of the upstream non-coding region, 9 bp of the first coding exon and 179 bp of the downstream intron. Samples were obtained from 52 unrelated non-HIV-1-infected and 99 HIV-1-infected Japanese, as well as from 122 non-HIV-1-infected and 112 HIV-infected Thais. Polymorphisms were identified at two positions: an A to G substitution at position −485 and an ATC deletion at a position from −29 to −27 upstream from the open frame ATG codon of the IL-7 gene (Fig. 1). Frequencies of these two polymorphisms are summarized in Table 1. As for the A to G mutation at position −485, there was no difference in frequency of the G allele between HIV-1-infected and non-HIV-1-infected individuals. For the allele of the ATC deletion, two of the 99 HIV-1-infected Japanese carried this allele, but none of the Thais. There was no linkage disequilibrium between these two mutations.

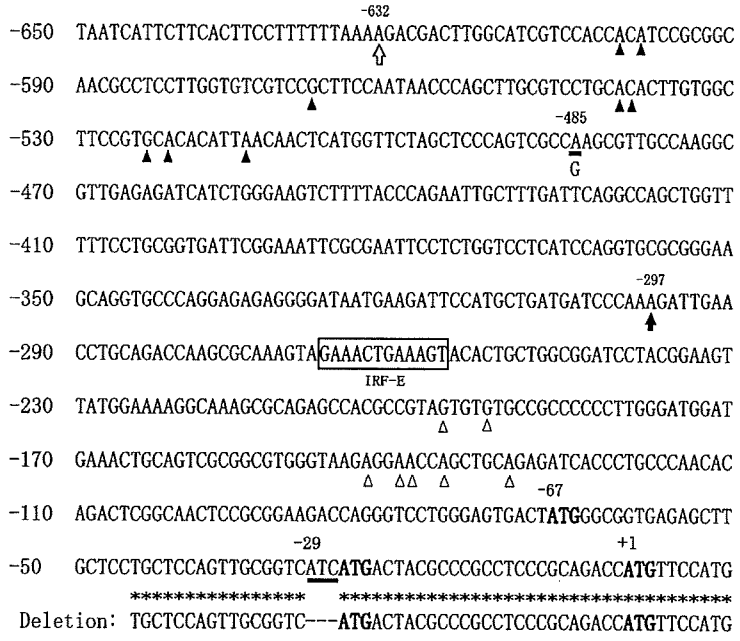

Figure 1. Fragment containing 650-bp of the upstream non-coding region and a part of the coding region of the IL-7 gene. Two polymorphisms, A to G at −485 and ATC deletion at −29 to −27 are underlined. The sequence with the ATC deletion is shown below the sequence without the ATC deletion. Asterisks denote sequence identity. Numbers denote positions from the initiation ATG of IL-7. An open arrow at −632 and a closed arrow at −297 denote the 5′ ends of the IL-7 upstream non-coding region inserted into reporter plasmids (see Figs 3 and 4). Triangles denote multiple transcription start sites that are clustered within the two distinct regions reported by Oshima *et al.* (2004). Open triangles denote transcription start sites specifically activated by IFN-γ. An open square denotes IRF-E (Oshima *et al.*, 2004).

In addition, calculation of nucleotide diversity in the 1470-bp fragment of the upstream non-coding region of IL-7 genes in all Japanese and Thai subjects showed 1.4×10^{-5} in Japanese and 0.9×10^{-5} in Thais. These results suggested that the human IL-7 gene has a highly conserved upstream non-coding region.

Roles of ATGs in the upstream non-coding region of IL-7 gene

In the upstream non-coding region, there are several out-of-frame ATGs (Fig. 1), with even the shortest transcript starting from position −130 containing two out-of-frame ATGs in the upstream non-coding region (Fig. 1). Because one of those out-of-frame ATGs occurred just downstream of the ATC deletion described previously, we then investigated roles of these upstream ATGs in IL-7 gene expression. For this purpose, we constructed a reporter plasmid in which the luciferase open reading frame was fused with the upstream ATG under the control of the upstream region of the IL-7 gene. As shown in Fig. 2, when a reporter plasmid carrying the region from position −632 to the authentic translation initiation ATG codon was transiently transfected into Jurkat or U937 cells, a significant increase in luciferase activity was observed, compared with the pGL3-basic vector employed as a control reporter plasmid in either cell, confirming a previous observation (Oshima *et al.*, 2004). When ATG at position −69 to −67 was fused with the luciferase open reading frame, luiferase activity became greatly enhanced (Fig. 2). These results indicated that the upstream AUG in IL-7 mRNA was more efficiently used for expression than the authentic AUG, and suggested that presence of upstream AUGs in IL-7 mRNA can be expected to reduce IL-7 translation levels.

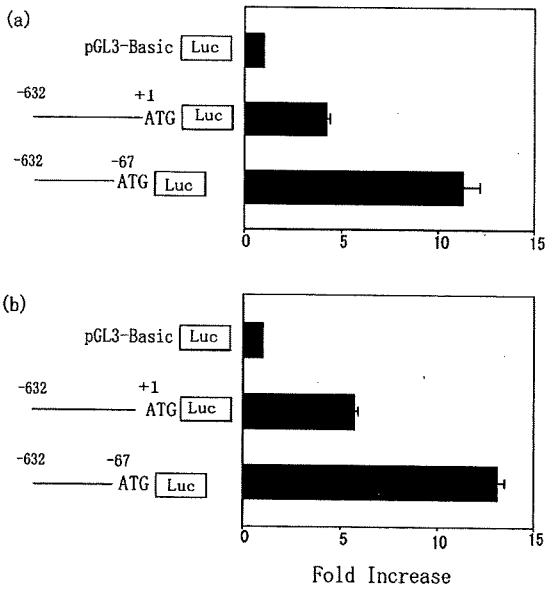

Figure 2. Luciferase activity mediated by the upstream non-coding region of the IL-7 gene. Jurkat (a) or U937 cells (b) were transfected with the plasmids indicated. The fold increase of each construct is represented by a bar. Data represent three independent experiments with similar results. Error bars show actual fluctuations among measurements of fold increase in four clones of each construct.

ATC deletion could affect the gene expression of IL-7

As mentioned previously, the ATC deletion occurred just upstream of the ATG located at position −26 to −24 (Fig. 1). Kozak previously reported that ACCATGG is

Table 1. Allele and genotype frequencies of A to G mutation at −485 and deletion mutation at −29 to −27 in HIV-1-infected and non-HIV-1-infected Japanese and Thai people

Japan					Thailand				
	HIV-1-Infected *n* (%)	Non-HIV-1-Infected *n* (%)		HIV-1-Infected *n* (%)	Non-HIV-1-Infected *n* (%)		HIV-1-Infected *n* (%)	Non-HIV-1-Infected *n* (%)
Allele			Genotype			Allele			Genotype		
A	196 (99.0)	102 (98.1)	AA	97 (98.0)	50 (96.2)	A	221 (98.7)	241 (98.8)	AA	109 (97.3)	119 (97.5)
G	2 (1.0)	2 (1.9)	AG	2 (2.0)	2 (3.8)	G	3 (1.3)	3 (1.2)	AG	3 (2.7)	3 (2.5)
			GG	0 (0)	0 (0)				GG	0 (0)	0 (0)
Total	198	104		99	52	Total	224	244		112	122
Allele			Genotype			Allele			Genotype		
W[a]	196 (99.0)	104 (100)	WW	97 (98.0)	52 (100)	W[a]	224 (100)	244 (100)	WW	112 (100)	122 (100)
D[b]	2 (1.0)	0 (0)	WD	2 (2.0)	0 (0)	D[b]	0 (0)	0 (0)	WD	0 (0)	0 (0)
			DD	0 (0)	0 (0)				DD	0 (0)	0 (0)
Total	198	104		99	52	Total	224	244		112	122

[a] W denotes the wild type at −29 to −27.

[b] D denotes deletion at −29 to −27.

the optimal sequence for translation initiation of preproinsuline by eukaryotic ribosomes and that substitution of G for A at position −3 (3-bp upstream from the ATG codon) reduced translation efficiency (Kozak, 1986). The A to G substitution at position −3 of an upstream, out-of-frame ATG condon also reportedly diminished translation from the corresponding upstream ATG and consequently increased translation from the authentic downstream ATG (Kozak, 1986). In the case of the human IL-7 gene, the sequence surrounding the ATG at position −26 to −24 is ATCATG but the ATC deletion observed in our study converted it into GTCATG (Fig. 1). These data indicate that the ATC deletion altered the A at position −3 into G (Fig. 1), thus hypothetically reducing translation efficiency from the upstream ATG at position −26 to −24 and increasing translation from the authentic IL-7 ATG. We therefore decided to test experimentally whether the ATC deletion polymorphism actually affected levels of expression from the authentic IL-7 ATG.

We constructed a reporter plasmid containing the upstream non-coding region from −632 to +3 with the ATC deletion and compared its luciferase activity with that of the wild-type version. As shown in Fig. 3(a), the reporter activity of the deletion mutant was approximately 30% higher than that of the wild-type plasmid. We also generated shorter versions of the wild type as well as mutant constructs carrying the upstream non-coding region from −297 to +3, which spans the minimal promoter region containing IRF-E (−268 to −257) (Oshima *et al.*, 2004). Again, the reporter activity of the deletion mutant was approximately 30% higher than that of the wild-type plasmid (Fig. 3b). We repeated the same experiments by using monocytic U937 cells. Here too, luciferase activity in the deletion mutant was approximately 25% higher than that in the corresponding wild-type plasmid when the upstream non-coding region of −632 to +3 was used (Fig. 4a). An approximately 20% increase in luciferase activity was observed in the deletion mutant when the upstream non-coding region −297 to +3 was used (Fig. 4c). It is known that INF-γ is capable of up-regulating the gene expression of IL-7 in intestinal epithelial cells through the IRF-E in the region −268 to −257 from the initiation ATG codon (Oshima *et al.*, 2004). As shown in Fig. 4(b,d), the addition of INF-γ to the transfected cells in fact did augment luciferase activity in U937 cells. Moreover, the deletion mutant exhibited significantly higher luciferase activity than the wild-type constructs (Fig. 4b,d). These results clearly indicate that ATC deletion in the upstream non-coding region resulted in higher expression from the authentic IL-7 ATG.

Discussion

In the study reported here, we demonstrated that an out-of-frame ATG in the upstream non-coding exon of IL-7 gene was more efficiently used for expression than the authentic ATG of IL-7 gene. We also found a naturally occurring ATC deletion polymorphism at position −29 to

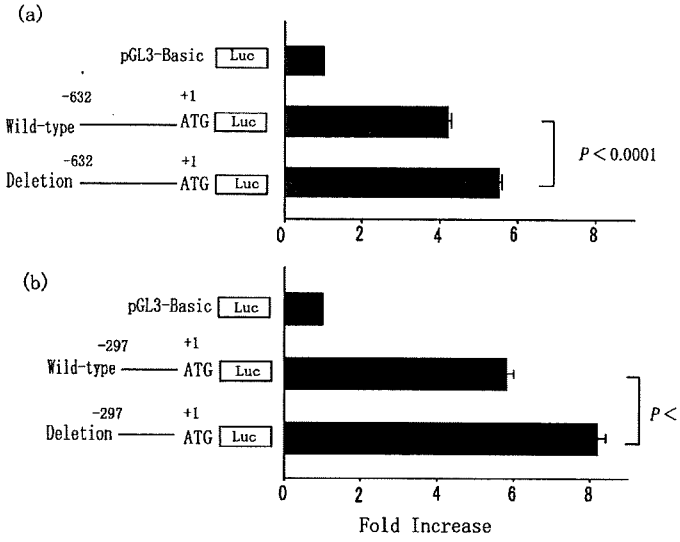

Figure 3. Luciferase activity mediated by the upstream non-coding region of the wild-type and ATC deletion in Jurkat cells. (a) A region from position −632 to +3 of the upstream non-coding region of the wild-type and ATC deletion. (b) A region from position −297 to +3 of the upstream non-coding region of the wild-type and ATC deletion. Data represent three independent experiments with similar results. Error bars show actual fluctuations among measurements of fold increase in four clones of each construct. *P* values for differences in fold increase are shown.

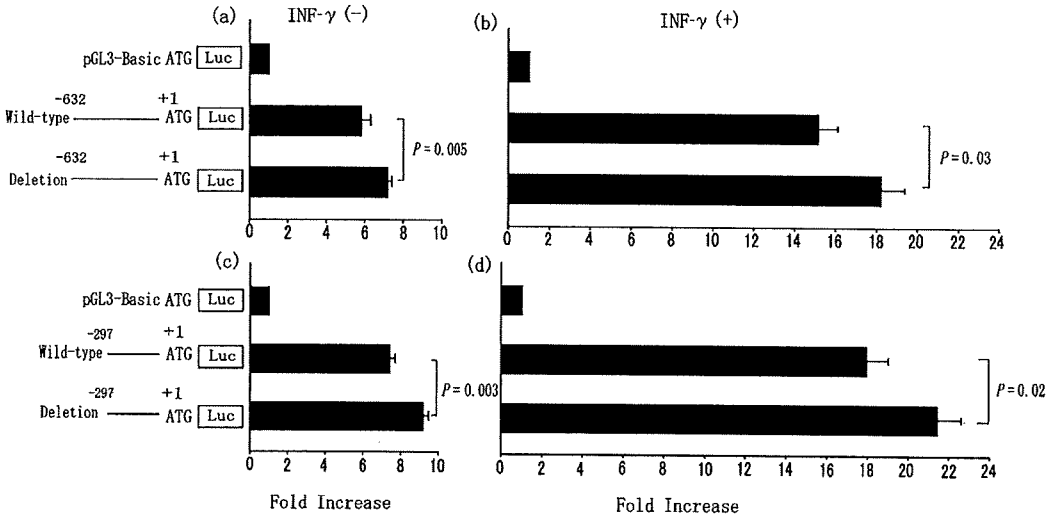

Figure 4. Luciferase activity mediated by the upstream non-coding region of the wild-type and ATC deletion in U937 cells. (a) A region from position −632 to +3 of the upstream non-coding region of the wild-type and ATC deletion without INF-γ. (b) A region from position −632 to +3 of the upstream non-coding region of the wild-type and ATC deletion with INF-γ. (c) A region from position −297 to +3 of the upstream non-coding region of the wild-type and ATC deletion without INF-γ. (d) A region from position −297 to +3 of the upstream non-coding region of the wild-type and ATC deletion with INF-γ. Data represent three independent experiments with similar results. Error bars show actual fluctuations among measurements of fold increase in four clones of each construct. *P* values for differences in fold increase are shown.

−27 in the upstream non-coding exon next to one of the upstream ATGs. This polymorphism was found to be capable of increasing the expression from the authentic IL-7 ATG in Jurkat T cell and U937 monocytic cell lines. This is the first time human genetic polymorphism has been identified that is supposed to affect expression of a protein by changing the translation efficiency from the out-of-frame AUG in the upstream non-coding region of mRNA.

There are a few precedents for a human genetic polymorphism near the initiation ATG codon affecting translation efficiency. A single nucleotide polymorphism (SNP) that switches C to T at position −1 upstream from the open frame ATG codon in the human annexin V gene has been found to increases translation efficiency and plasma levels of annexin V, and to decreases the risk of early myocardial infarction (Gonzalez-Conejero *et al.*, 2002). Also, an SNP that switches G to T at position −3 upstream from the open frame ATG codon of the BRCA1 gene in sporadic breast cancer causes down-modulation of translation efficiency (Signori *et al.*, 2001). Moreover, a mutation of G into A at +4 downstream from the open frame ATG codon of the human androgen receptor gene observed in

